

1L7801265

LS-276

**NUCLEAR DATA AND LOW ENERGY
NUCLEAR RESEARCH IN ISRAEL**

**Progress Report
for 1977**

compiled by
SHIMON YIFTAH

Israel Atomic Energy Commission

AVAILABILITY

Israel Atomic Energy Commission reports and
bibliographies may be obtained on application to:

TECHNICAL INFORMATION DEPARTMENT
ISRAEL ATOMIC ENERGY COMMISSION

P. O. B. 17120
TEL-AVIV, ISRAEL

NUCLEAR DATA AND LOW ENERGY
NUCLEAR RESEARCH IN ISRAEL

Progress Report
for 1977

compiled by
SHIMON YIFTAH

Israel Atomic Energy Commission

July 1978

C O N T E N T S

	<u>Page</u>
Introduction.....	1
The Weizmann Institute of Science.....	2
Israel Atomic Energy Commission Laboratories.....	14
Universities.....	50
Author Index.....	55

2 2

The Israel Nuclear Data and Low Energy Nuclear Research relevant to the International Nuclear Data Committee was continued in the various institutions listed in previous Progress Reports (LS-270 for 1976).

The latest major experimental facility, the 14 UD pelletron, was installed in the Koffler Accelerator Tower at the Weizmann Institute of Science, Rehovot, and accepted on April 1st 1977. A report in Revue de Physique Appliquee of October 1977 including a description of the facility, acceptance performance, as well as some supplementary devices, is reproduced in the beginning of this report.

Brief abstracts of the research work, both published and unpublished, are presented in the following pages.

The Weizmann Institute of Science

Department of

NUCLEAR PHYSICS

THE KOFFLER ACCELERATOR IN REHOVOT

G. GOLDRING

The Weizmann Institute of Science, Rehovot, Israël

Résumé. — Le nouvel accélérateur 14UD à Réhovot a été réceptionné le 1.4.77. On décrit ses caractéristiques de fonctionnement ainsi que divers équipements supplémentaires, le sélecteur de charge au terminal, la source d'ions à *sputtering* et le hacheur-groupeur.

Abstract. — The new 14UD accelerator in Rehovot has been accepted on april 1st, 77. The acceptance performance is described, as well as some supplementary devices : the terminal charge selector, the sputtering ion source and the chopper-buncher.

I would like to start this presentation with a short survey of the history of our project. The main events are outlined in figure 1. Altogether the project took seven years from the moment the first tentative ideas came up, to completion. Two years were spent on deciding on specific goals and a plan of operation as well as getting the project approved and funded. The technical planning took about a year and a half and the construction of the building three and a half years. This period includes a six months' break caused by the october war. The assembly of the accelerator proper and the testing of the machine took about sixteen months, mostly overlapping with the construction work.

The accelerator as it stands now is a standard 14 UD Pelletron of the NEC company with the following additions and innovations :

1. Enclosed corona tubes for the voltage distribution along the HV structure. There are four tube systems in all : one each for the stack and the acceleration tubes, in the low energy and high energy sections.
2. An enlarged terminal with a total length of 3.6 meters for the installation of beam optical equipment which will be described later.

3. A dead section in the middle of the LE tube, housing an electrostatic quadrupole triplet and a vacuum pump. The performance of the accelerator in the acceptance tests is summarized in table I.

Some additional points relating to the test runs are worth mentioning :

1. The proton beam transmission through the accelerator was about 90 %.
2. The short term voltage stability, without any feedback correction, was at least as good as the voltmeter read-out accuracy — about 10 kV — over the entire range up to 14 MV.

A number of additions to the accelerator are planned and we hope to install them in the course of the coming year. They are summarized in table II.

The charge selector is part of a general policy to transmit the entire beam through the accelerating tubes and to keep it clear of the tube electrodes. The overall optical plan of the Pelletron is shown in figure 2. The charge selector was devised for work with heavy ions. It acts as a filter transmitting one and only one charge state out of the mixture

TABLE I
Acceptance test performance

Particle	Voltage MV	Stripper	Final energy MeV	Beam current on Faraday cup after analysing magnet
p	4	C-foil	8	3 μ A
p	9	C-foil	18	5
p	14	C-foil	28	3
Cl	14	C-foil	140	50 pA
Cl	14	nitrogen	112	50

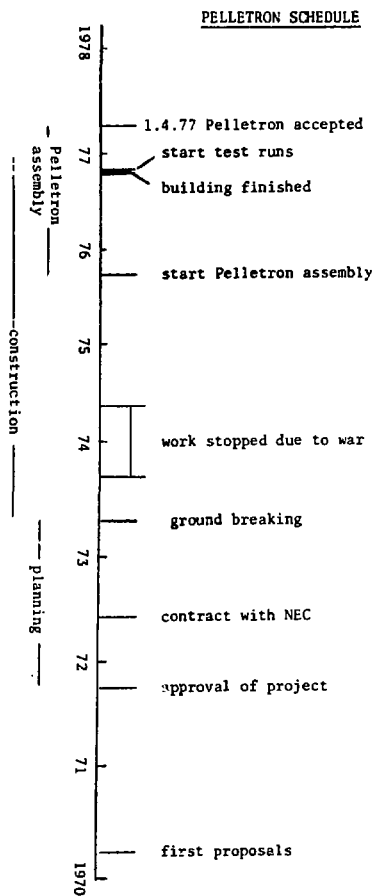


FIG. 1. — Pelletron schedule.

TABLE II

Additions to the Pelletron

Equipment	Objective
1. General Ionex sputtering source	Large variety of available ions.
2. Charge selector in HV terminal	Heavy ion beams of high energy and high intensity.
3. Chopper-buncher	Beam pulses of less than 100 ps.

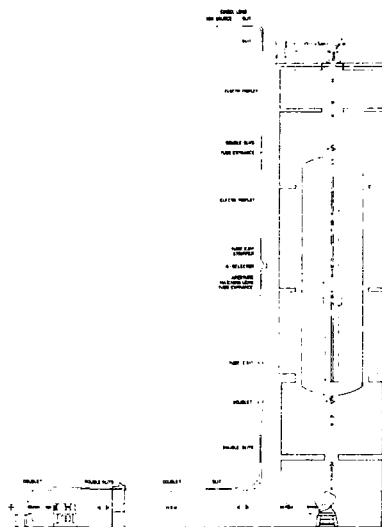


FIG. 2. — General layout of the Pelletron and the beam transport system.

emanating from the stripper. The charge selector was designed and developed in our laboratory by Z. Segalov and E. Skurnik from our Laboratory following a suggestion by D. Larson who worked with us on the beam optics of the accelerator installation. The instrument is a quadrupole triplet with each of the three elements displaced from the optical axis, causing the selected charge to be transmitted on-axis and focussed on an aperture behind the selector, while other charges are defocussed and deflected (Fig. 3). The biggest uncertainty in the projected operation of the selector was the beam aberration and its possible effect on the intensity and the quality of the transmitted beam. In the course of the development work it was ascertained that under certain conditions the aberrations were small and essentially insignificant. Following this work an operational instrument has been manufactured by NEC. This has now been shipped to us and we expect to install it in the course of the next six months. A schematic view of the HV terminal incorporating the charge selector and its associated matching lens is shown in figure 4. The charge selector will be operated through standard NEC lucite control rods and the beam diagnosis will be effected through a beam profile monitor and a retractable Faraday cup, with their outputs transmitted to the outside through an optical link.

Figures 5 and 6 portray two instances of the excep-

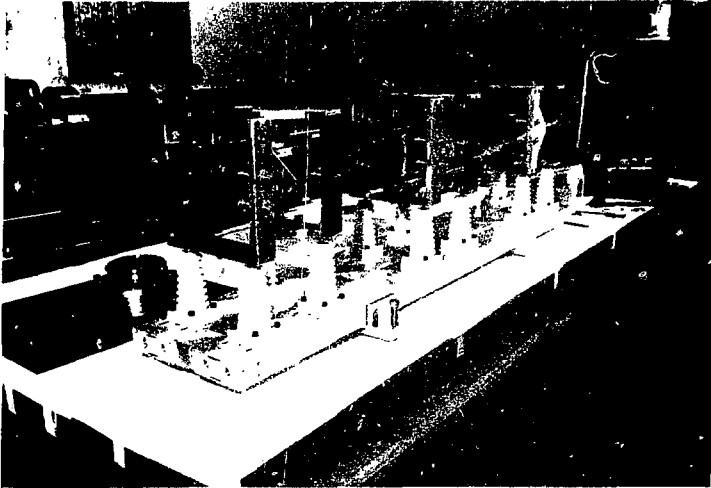
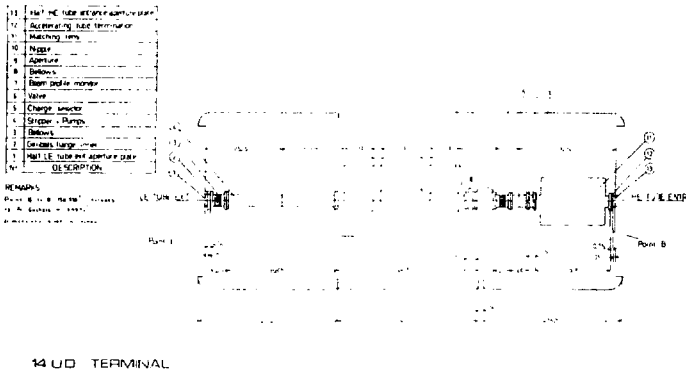


FIG. 1. Photograph of the work benches of the charge selector in the vacuum envelope.



14 UD TERMINAL

FIG. 2. Schematic diagram of the charge selector.

ted performance of the charge selector, based on measurements on the model with a proton beam.

The chopper buncher is a system designed by I. Ben Zvi from our laboratory with the objective of obtaining short beam pulses with a width of less than 100 ps. It is intended for velocity selection of particles emitted in nuclear reactions. The system is shown schematically in figure 7. The first element is an automatic electrostatic chopper (Fig. 8) of a design pro-

posed first proposed by Zecher. This design is free of the velocity spread introduced in the operation of conventional choppers (scintilator deflectors). The chopper is followed by a conventional pre-buncher situated inside the accelerator tank immediately before the low energy tube in order to minimize the effect of the velocity inhomogeneity in the beam. The buncher is made of two parts operating at the fundamental frequency of 4 MHz and the third harmonic. The

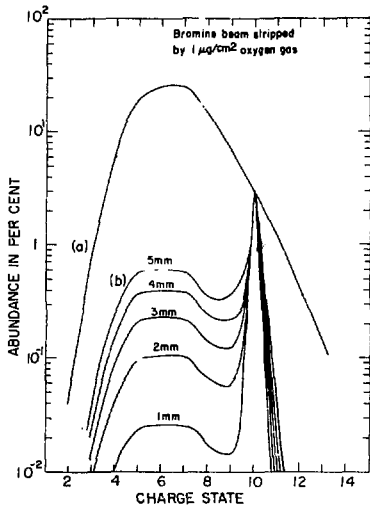


FIG. 5. — Selection quality of an offset triplet charge selector for a 14 MeV bromine beam stripped by $1 \mu\text{g}/\text{cm}^2$ oxygen gas leading to an angular divergence of ± 3 mrad. The initial beam width at the object plane is 1 mm. (a) Equilibrium charge state distribution after stripping. (b) Charge state distribution after selection for the various image apertures marked on the curves.

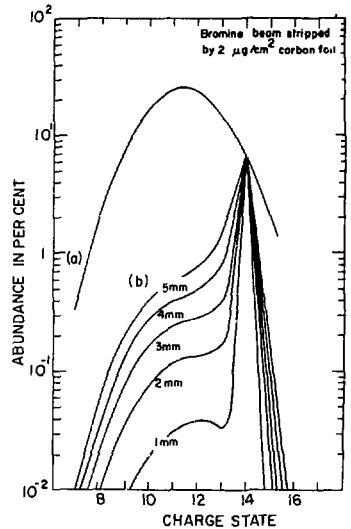


FIG. 6. — Similar to figure 5, for carbon foil stripper of $2 \mu\text{g}/\text{cm}^2$.

ensuing beam pulses are spaced 250 ns apart. The most important and novel element is a klystron buncher made out of two superconducting doubly re-entrant niobium cavities operating at 430 MHz situated in close proximity (~ 2 meters) to the target. The superconducting buncher is shown in figure 9 and the cavities are shown in figure 10. Computed intensity distributions after the analysing magnet and at the target position are shown in figures 11 and 12.

I would like to conclude with a few remarks concerning the organization of the installation and assembly of the accelerator and other work in the laboratory during that time. Our laboratory has one target area and one control room. They are common to both the old EN tandem and the new Pelletron accelerator. The plan of the ground floor of the laboratory is shown in figure 13. With the new accelerator it was found necessary to introduce some modifications in these rooms and in the equipment housed in them (e.g. upgrading the vacuum equipment). Throughout this period we endeavoured to interfere as little as possible with the experimental work conducted with the EN tandem; modifications in the target area were concentrated in a few relatively short periods that were scheduled well in advance. Operators were available

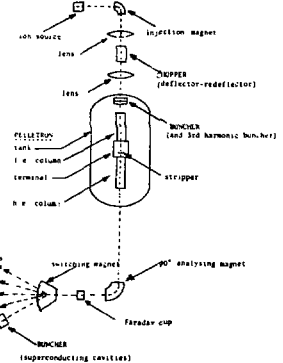


FIG. 7. — Chopper-buncher system.

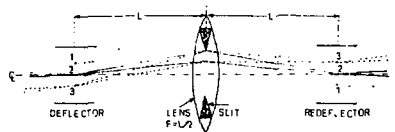


FIG. 8. — Schematics of the achromatic electrostatic beam chopper.

THE KOFFLER ACCELERATOR IN REHOVOT

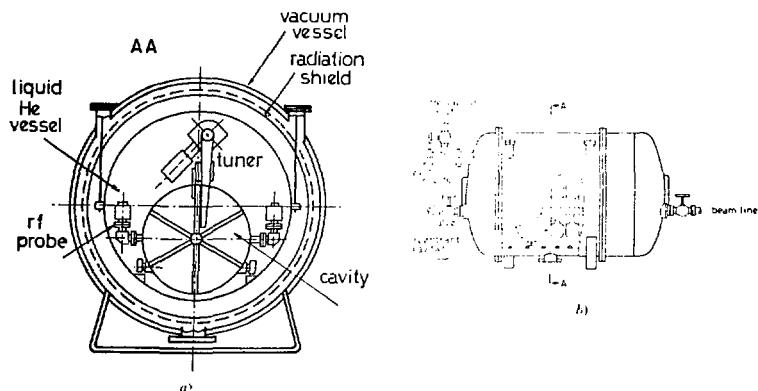


Fig. 9 Superconducting buncher

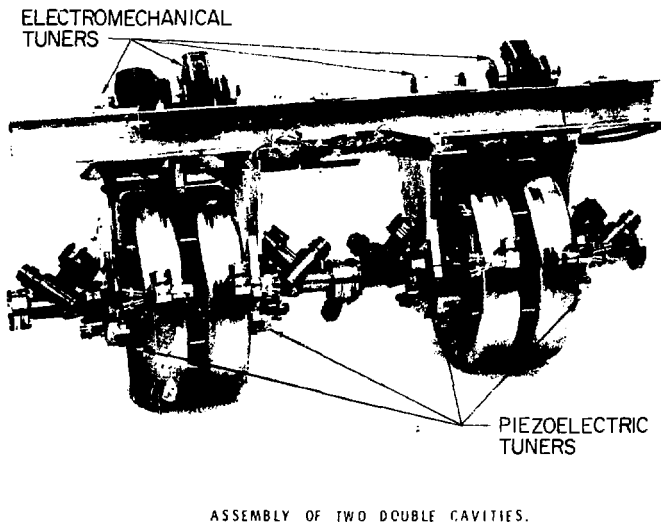
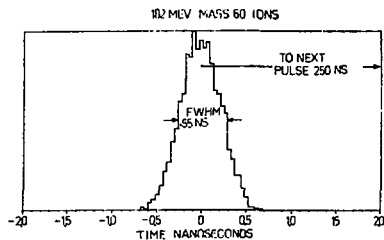


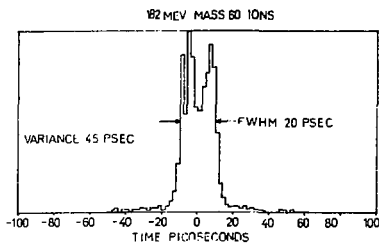
FIG. 10. - The niobium cavities of the buncher (The structure shown is an acceleration device assembled at Stanford university. Only one double cavity will be used in the buncher.)

REVUE DE PHYSIQUE APPLIQUÉE



DISTRIBUTION OF 6370 PARTICLES PER ANALYSIS MAGNET

FIG. 11. — Calculated beam intensity distribution at the position of the stabilizing slit (or the Faraday cup Fig. 7), exhibiting the action of the chopper and the pre-buncher.



DISTRIBUTION OF 6370 PARTICLES AT THE TARGET AREA

FIG. 12. — Calculated beam intensity distribution at the position of the target exhibiting the action of the full bunching system. The peak comprises about 15 percent of the total beam issuing from the ion source. The time between pulses is 250 ns.

on an on-call basis to help with the running of the tandem through two shifts although all the technicians were heavily involved in the installation of the Pelletron.

The first experiments on the Pelletron were started last week. In the year to come our technical crew will still be very much involved with the various modifications and additions that I have indicated and in that period we plan to have alternating six week periods of 14 UD and EN operation so that there will be ample prescheduled time for development work on the Pelletron and at the same time there will, hopefully, always be one accelerator available for experiments.

The very first experiment on the Pelletron was a study of the Coulomb explosion of the OH^- mole-

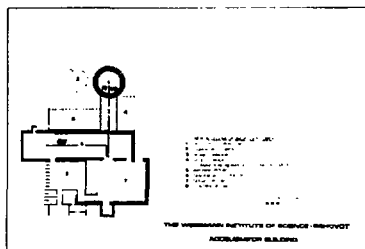


FIG. 13. — Plan of the ground floor of the laboratory.

cular ion as it dissociates in the strippers in the terminal of the Pelletron. The measurements were conducted at constant terminal voltage using the 90° magnet as a spectrometer.

In a control measurement an H^+ beam of 24 MeV was analysed and the result is shown in figure 14. The

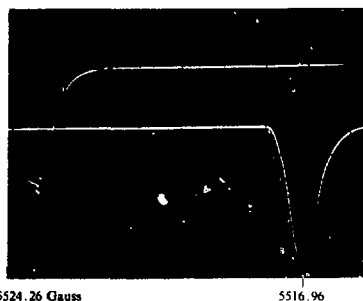


FIG. 14. — Magnetic analysis of an H^+ beam of 24 MeV issuing from the Pelletron. The duration of the sweeps across the H^+ line was about 1 s. The peak positions in the two sweeps are at 5524.26 gauss and 5516.96 gauss.

sweep across the H^+ line took about 1 s. The width and the shape of the line is consistent with the magnet slit apertures and it can therefore be surmised that in the short term the energy homogeneity in the Pelletron beam is better than the line width which is $\sim 5 \times 10^{-4}$ in $\Delta E/E$ (FWHM). Over longer period (of several minutes) the line was found to spread about two or three times as much.

Prompt γ rays emitted in fission of ^{226}Ra by 12 MeV protons

A. Gayer and Z. Fraenkel

Weizmann Institute of Science, Rehovot, Israel

(Received 14 February 1977)

The total energy associated with the emission of prompt γ rays in fission of ^{226}Ra induced by 12 MeV protons was measured in correlation with the fragment mass and kinetic energy. The dependence of the average total γ -ray energy on fragment mass and total kinetic energy resembles the corresponding dependence of the average number of neutrons. Using these results and the results for the average number of neutrons, we calculated the excitation energy of the fragments at the scission point. The results support the view that the scission-point configuration for the symmetric fission mode is more elongated than that for the asymmetric mode.

[NUCLEAR REACTIONS, FISSION $^{226}\text{Ra}(p, f)$, $E=12$ MeV; measured coin. fragment energy, γ -ray energy at 0° with respect to fragment; deduced total γ -ray energy emitted from the fission fragments.]

Direct measurement of prompt neutrons emitted in fission of ^{226}Ra by 12 MeV protons

A. Gayer and Z. Fraenkel

Weizmann Institute of Science, Rehovot, Israel

(Received 14 February 1977)

Prompt neutron energy distributions were measured at 0° and 90° with respect to the fission axis, in correlation with the mass-energy distribution of the fragments, for the fission of ^{226}Ra induced by 12 MeV protons. The average number and average kinetic energy of pre-fission and post-fission neutrons were obtained as a function of fragment mass and total kinetic energy. The average number of pre-fission neutrons emitted is 0.33 ± 0.15 n/fission (this includes also contributions from scission neutrons). By comparing this result with calculations of the average number of "true" pre-fission neutrons, it was found that the number of true pre-fission neutrons is zero. The average number of post-fission neutrons emitted from both fragments is 3.20 ± 0.20 with an average kinetic energy of 1.33 ± 0.07 MeV. The dependence of the number of post-fission neutrons on the fragment mass can be interpreted as a combination of a sawtooth structure for the asymmetric mass division and a linearly increasing function for the symmetric mass division.

[NUCLEAR REACTIONS, FISSION $^{226}\text{Ra}(p, n/f)$, $E=12$ MeV; measured coin. fragment energy, neutron velocity at $\theta=0^\circ, 90^\circ$ with respect to fragment; deduced number and kinetic energy of pre-fission, post-fission neutrons.]

2.B:2.N

Nuclear Physics A291 (1977) 459-474; © North-Holland Publishing Co., Amsterdam
Not to be reproduced by photoprint or microfilm without written permission from the publisher

**TOTAL FUSION CROSS SECTIONS FOR $^{18,17,16}\text{O} + ^{27}\text{Al}$
AT ENERGIES NEAR THE COULOMB BARRIER †**

Y. EISEN, I. TSERRUYA, Y. EYAL^{††}, Z. FRAENKEL and M. HILLMAN^{†††}
The Weizmann Institute of Science, Rehovot, Israel

Received 2 May 1977
(Revised 28 July 1977)

Abstract: Total fusion cross sections have been measured for $^{18,17,16}\text{O} + ^{27}\text{Al}$ systems at bombarding energies 27-42 MeV. The evaporation residues were detected in the angular range 4° - 25° (lab) using a ΔE - E counter telescope. Barrier radii extracted from total fusion and elastic scattering cross sections are found to increase with the projectile mass. The effect of the yrast levels on the isotopic yields in the evaporation cascade is investigated.

E

NUCLEAR REACTIONS $^{27}\text{Al}(^{18}\text{O}, \text{X}), (^{17}\text{O}, \text{X}), (^{16}\text{O}, \text{X}), E = 27-42$ MeV; measured complete fusion $\sigma(E)$. $^{27}\text{Al}(^{16}\text{O}, ^{16}\text{O}), (^{17}\text{O}, ^{17}\text{O}), (^{18}\text{O}, ^{18}\text{O}), E = 21-40$ MeV. Measured $\sigma(E, \theta)$; deduced effective fusion radii.

2.N

Nuclear Physics A287 (1977) 353-361; © North-Holland Publishing Co., Amsterdam
Not to be reproduced by photoprint or microfilm without written permission from the publisher

**COMPOUND TRANSFER AND DIRECT TRANSFER REACTIONS
INDUCED BY ^{17}O ON ^{13}C**

R. CHECHIK, Z. FRAENKEL, H. STOCKER † and Y. EYAL ††
Department of Nuclear Physics, The Weizmann Institute of Science, Rehovot, Israel

Received 25 April 1977

Abstract: The elastic scattering, inelastic scattering, single-neutron transfer reactions $^{13}\text{C}(^{17}\text{O}, ^{16}\text{O})^{13}\text{C}$, $^{13}\text{C}(^{17}\text{O}, ^{18}\text{O})^{13}\text{C}$ and $^{13}\text{C}(^{17}\text{O}, ^{18}\text{O}_2 +, 1.99)^{13}\text{C}$, and seven other exit channels which involve ^7Li , ^9Be , ^{11}B and ^{13}N have been measured for the system $^{17}\text{O} + ^{13}\text{C}$ at 12.9 and 14 MeV c.m. It is shown that all reactions mentioned above have significant contributions from compound nuclear decay, following fusion of projectile and target.

E

NUCLEAR REACTIONS $^{13}\text{C}(^{17}\text{O}, ^{17}\text{O})(^{17}\text{O}, ^{17}\text{O}), (^{17}\text{O}, ^{18}\text{O}), (^{17}\text{O}, ^{16}\text{O}), (^{17}\text{O}, ^{13}\text{N}), (^{17}\text{O}, ^{12}\text{F}), (^{17}\text{O}, ^{21}\text{Ne}), (^{17}\text{O}, ^{23}\text{Na}), E(\text{c.m.}) = 12.9, 14$ MeV; measured $\sigma(\theta)$; deduced reaction mechanisms 95% ^{13}C enriched targets.

DYNAMIC EXCITATION IN FISSION

T. LEDERGERBER*, Z. PALTIEL and Z. FRAENKEL

The Weizmann Institute of Science, Rehovot, Israel

and

H. C. PAULI

Max-Planck-Institut für Kernphysik, Heidelberg, Germany

Received 6 September 1976

Abstract: The excitation mechanism of the fission process is studied in terms of a model of particles moving in a deformed time-dependent potential. A residual interaction of the pairing type is incorporated by means of the BCS approximation. Only two-quasi-particle excitations up to some cutoff energy are included. The separation of the total excitation energy into intrinsic and translational parts is made at the scission point. The present calculations for ^{240}Pu show that, in the framework of this model, most of the available energy at scission is transformed into intrinsic excitation energy. However the convergence of the calculated value for the cutoff energy is unsatisfactory, and hence a description in terms of a better model space is needed. The fact that very many channels are involved suggests that a statistical treatment may be useful.

Study of the Breakup of Fast OH^- Ions Passing through Carbon Foils and Nitrogen Gas

A. Faibis, G. Goldring, and Z. Vager

Department of Nuclear Physics, The Weizmann Institute of Science, Rehovot, Israel

(Received 28 July 1977)

OH^- ions were injected into a "Pelletron"-type tandem electrostatic accelerator and dissociated in the high-voltage terminal by passage through gas and foil strippers. The dissociated protons were further accelerated and their energy spectrum was analyzed in a 90° magnet. The ions stripped in foils exhibit the effects of a Coulomb explosion and a wake field. The stripping in gas appears to be of a different character. An explanation of this difference is proposed, based on the assumption of a strictly sequential removal of electrons from the ions.

WIS-77/16 Ph

Elastic Scattering of $^{17,18}\text{O}$ on $^{12,13}\text{C}$ at $E_{\text{c.m.}} = 12.6 - 14.0$ MeV

R. Chechik, Y. Eyal, H. Stocker* and Z. Fraenkel

Department of Nuclear Physics
The Weizmann Institute of Science
Rehovot, Israel

ABSTRACT

The angular distributions of the elastic scattering of $^{17,18}\text{O}$ on $^{12,13}\text{C}$ were measured at center-of-mass energies between 12.6 to 14.0 MeV. A rise of the cross section at backward angles was observed. Standard optical-model fits were found to reproduce reasonably well the forward part of the cross section, but fail at backward angles. Possible contributions of first-order cluster exchange and compound-nucleus reactions are discussed. Excitation functions of various exit channels in the $^{18}\text{O} + ^{12}\text{C}$ system were measured at backward angles in the energy range of 12.0 to 14.8 MeV c.m. No significant correlation was found between any of these cross sections.

NUCLEAR REACTIONS: $^{12}\text{C}(^{17}\text{O}, ^{17}\text{O})^{12}\text{C}$, $^{12}\text{C}(^{18}\text{O}, ^{18}\text{O})^{12}\text{C}$, $^{13}\text{C}(^{17}\text{O}, ^{17}\text{O})^{13}\text{C}$,
 $^{13}\text{C}(^{18}\text{O}, ^{18}\text{O})^{13}\text{C}$. $E = 12.6 - 14.0$ MeV c.m.;
measured $\sigma(\theta)$; deduced optical-model parameters.
Natural ^{12}C targets, 95% enriched ^{13}C targets.

* Present address: Atomic Energy Control Board, Ottawa, Ont., Canada

Israel Atomic Energy Commission
Laboratories

Evaluated Delayed Neutron Spectra and Their Importance in Reactor Calculations*

D. Saphier

Argonne National Laboratory, 9700 South Cass Avenue, Argonne, Illinois 60439

D. Ilberg

Soreq Nuclear Research Centre, Yavne, Israel

S. Shalev

*Julius Silver Institute of Bio-Medical Engineering
Technion-Israel Institute of Technology, Haifa, Israel*

and

S. Yiftah

Soreq Nuclear Research Centre, Yavne, Israel

Received July 28, 1976

Delayed neutron emission spectra from thermal-neutron fission of ^{233}U , ^{235}U , ^{239}Pu , and ^{241}Pu , from fast-neutron fission of ^{232}Th , ^{235}U , ^{238}U , and ^{239}Pu and from high-energy neutron (14.7-MeV) fission of ^{235}U and ^{238}U , for six groups of delayed neutrons are evaluated. The evaluation is based on recent measurements of delayed neutron spectra from 20 fission product isotopes. The data are presented in graphic form and are compared to directly measured equilibrium spectra whenever available. Tables with a convenient 54-energy-group structure are provided to facilitate their use in reactor calculations. The results of a limited number of two-dimensional, multigroup, transient calculations for the Clinch River Breeder Reactor core, using the newly evaluated spectra, are compared with calculations using some older spectra. The importance of the inclusion of these data in reactor dynamic calculations is evaluated.

* This paper received the American Nuclear Society Meritorious Service Award as the best publication in Reactor Physics in Nuclear Science and Engineering for the years 1975-1977.

Curium-244 Neutron Data Evaluation

M. Caner and S. Yiftah

Abstract

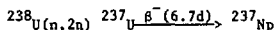
An evaluation of neutron nuclear data was performed for the isotope curium-244. The energy range covered was 10^{-3} eV to 15×10^6 eV. All significant cross sections were considered.

In the resolved resonance range, a maximum likelihood method was developed for the area analysis of underdetermined data. In the fast neutron energy range, spherical optical model and statistical theory calculations were done. The (n, xn) cross sections were calculated using a formalism based on compound nucleus decay with an improved treatment of $(n, 3n)$ competition.

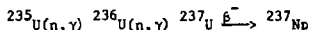
EVALUATION OF ^{237}Np MICROSCOPIC NEUTRON DATA

S. Waxler*, M. Caner and S. Yiftah

An evaluation of the following ^{237}Np neutron cross sections: total, elastic, radiative capture, fission, total inelastic, partial inelastic, (n,2n), (n,3n) and differential elastic, was made from 10^{-3} eV to 15×10^6 eV. The number of neutrons per neutron-induced fission and the average elastic scattering cosine in the lab system were also evaluated. The experimental data were supplemented by optical model and statistical theory calculations⁽¹⁾. The evaluated data were compared with the ENDF/B-IV file (MAT 1263). ^{237}Np is the only isotope of neptunium which is stable against beta decay. It has an alpha decay half-life of 2×10^6 years. In reactors with moderate ^{235}U enrichment it is produced through the reaction



In highly enriched reactors it is produced through the reaction



The knowledge of ^{237}Np neutron cross sections is important for thermal reactor calculations and actinide recycle calculations.

REFERENCE:

1. Caner, M. and Yiftah, S., Nucl. Sci. Eng. 59, 46 (1974)

COMPARATIVE ANALYSIS OF RECENT AMERICAN, GERMAN AND RUSSIAN EVALUATED NUCLEAR DATA FILES

Y. Gur and S. Yiftah

The American ENDF/B-IV, the German KEDAK-3 and the Russian SOKRATOR evaluated nuclear data files were compared. A preliminary comparison of the ^{235}U , ^{238}U and ^{239}Pu nuclear data on the microscopic cross section level revealed significant differences^(1,2). As a consequence, an error in KEDAK and a number of errors in SOKRATOR were detected. The error in KEDAK will be corrected in its next versions.

Significant differences were found in the resonance files of the three libraries. Graphical displays of smooth cross sections above 100 keV disclosed probable errors in SOKRATOR in the ^{239}Pu fission cross section and 12% differences in the ^{238}U capture cross sections. Although the capture cross

*Technion, Israel Institute of Technology, Haifa

section itself is small in all three files, the variations between the files will influence the computed breeding ratio.

Considerable differences were also found in the inelastic scattering cross sections. These are particularly significant since inelastic scattering is the main process by which fast neutrons are slowed down by heavy elements.

The SOKRATOR data for ^{235}U were translated to ENDF/B format and the multigroup cross sections were computed. The KEDAK data will also be translated and the multigroup cross sections and nuclear systems will be computed and compared so that the dependence of the physical parameters upon the basic data file will be established.

REFERENCES:

1. Gur, Y. and Yiftah, S., in: Trans. Nucl. Soc. Israel, vol. 4, 1976, p.12.
2. Ibid, p.15.

A COMPARISON OF SOME EIGENVALUES IN REACTOR THEORY⁽¹⁾

Y. Ronen, D. Shvarts and J.J. Wagschal*

A comparison was made of the limitations of the eigenvalues for the effective neutron multiplication factor per neutron generation k , the multiplication factor per collision γ , and the fundamental multiplication rate, as they concern the neutron spectrum and the spectral properties of the integral transport operators. Numerical examples of analyses of fast neutron plutonium systems were given. Consideration of the advantages of the rarely used γ eigenvalue led to the conclusion that it should be used more often.

REFERENCE:

1. Ronen, Y., Shvarts, D. and Wagschal, J., J. Nucl. Sci. Eng. 60, 97 (1976)

YIELDS OF Rb, Cs, Sr AND Ba ISOTOPES IN THERMAL FISSION OF ^{235}U

M. Schmid, Y. Nfir-El, G. Engler and S. Amfel

An integrated surface ionization target-ion source assembly of the SOLIS system^(1,2), highly efficient for alkali and alkaline earth elements, was used to measure Kb, Cs, Sr and Ba yields in thermal neutron fission of ^{235}U .

The beta activity was scanned over the mass interval 89-99 for Rb, 138-148 for Cs, 92-100 for Sr and 141-149 for Ba isotopes. The separated isotopes were collected on a moving tape which permitted the removal of background activity. The beta activity was measured using a 300 μm silicon surface barrier detector. Figure 1 shows a typical activity scan.

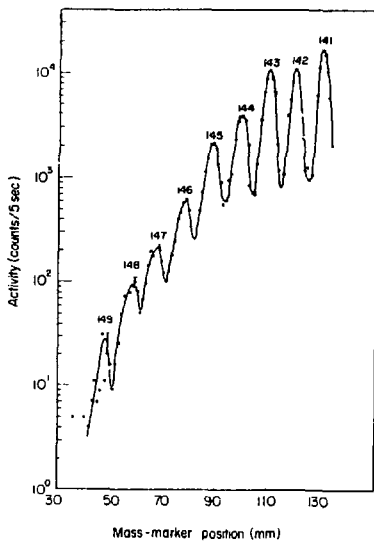


Fig. 1

Beta activity scan over the mass range 141-149

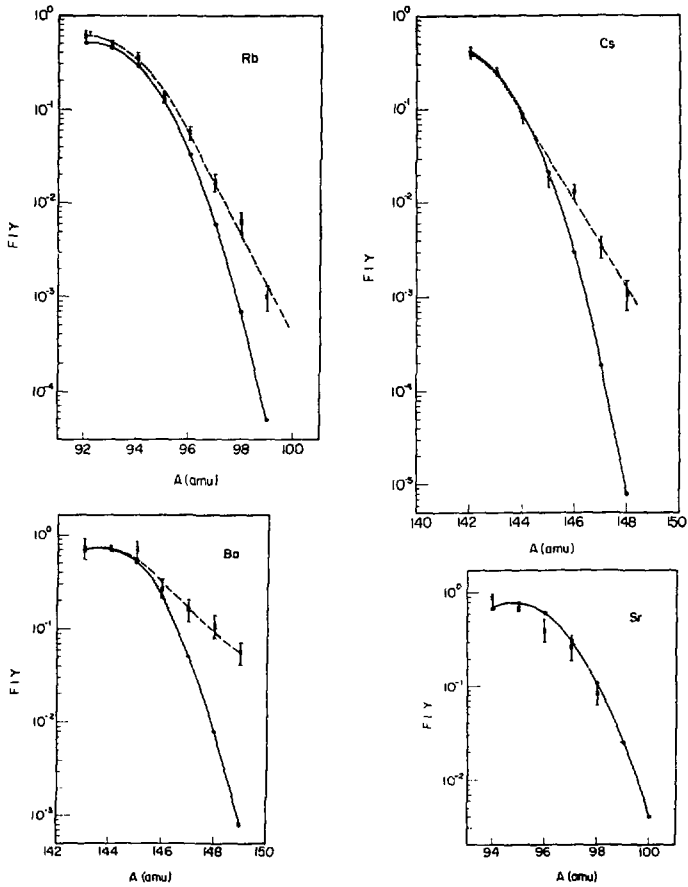


Fig. 2
Fractional independent fission yields for Rb, Cs, Sr and Ba isotopes.
X experimental points • determined by odd-even systematics ⁽³⁾

Fission yields were calculated by decomposing the activity scan into its isotope components. This was done by fitting each component to a Gaussian by a least squares computer code. Corrections were made by taking into account radioactive decay of the products and their delay times in the source as well as contributions by parent and daughter nuclides. Figure 2 show the distribution of independent fission yields of Rb, Cs, Sr and Ba isotopes, respectively. The yields of $^{98,99}\text{Rb}$, $^{146-148}\text{Cs}$ and $^{145-149}\text{Ba}$ were measured for the first time. The isotopes $^{147,148}\text{Cs}$ were identified for the first time.

A comparison of the measured fission yields with the values predicted by the odd-even systematics of Amiel and Feldstein⁽³⁾ showed agreement in the peak of the isotope yield distribution curves, but in the wings of the curve the measured yields were higher than the predicted values, as can be seen in Fig. 2. A theoretical study of this phenomenon is in progress.

REFERENCES:

1. Shmid, M., Nir-El, Y., Engler, G. and Amiel, S., previous article, this annual report.
2. Amiel, S., Engler, G., Nir-El, Y. and Shmid, M., Nucl. Instrum. Methods 139, 305 (1976)
3. Amiel, S. and Feldstein, H., Phys. Rev. C11, 845 (1975)

ISOMER YIELD RATIOS OF ^{132m}I and ^{134m}I (1)

N. Lavi and Y. Nir-El

The high spin isomers ^{132m}I and ^{134m}I were produced, detected and measured in the thermal neutron induced fission of ^{235}U . The decay curve shown in Fig. 3

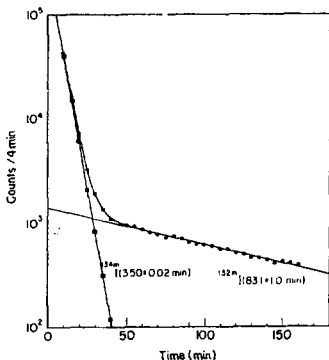


Fig. 3
Decay curve of the 28.6 keV K_{α} line
of iodine

was obtained by following the decrease of the 28.6 keV K_{α} peak of iodine. The two components were obtained by a least squares analysis. The half-lives of ^{132m}I and ^{134m}I were found to be 83.1 ± 1.0 min and 3.50 ± 0.02 min, respectively. Good agreement was found between the experimental ratio of yields and the predicted ratio based on the charge distribution in fission.

REFERENCE:

1. Lavi, N. and Nir-El, Y., J. Inorg. Nucl. Chem. 38, 2133 (1976)

DELAYED NEUTRON EMISSION PROBABILITIES OF Rb AND Cs ISOTOPES

G. Engler, E. Ne'eman*, S. Shalev**, Y. Nir-El and M. Shmid

Delayed neutron emission probability (P_n) studies of Rb and Cs isotopes are currently in progress at the Soreq on-line isotope separator facility SOLIS. A direct technique based on simultaneous determination of the total number of neutrons and beta activity from precursor nuclei is being used. The neutron counting system consists of 12 BF_3 proportional counter tubes which are embedded in a block (80x80x80 cm) of polyethylene and arranged in a concentric ring about a central hole. The central hole accommodates the ion beam tube at the end of which is a 300 μm surface barrier solid state beta detector. The beta detector is positioned very close to a moving tape which permits the removal of background activity. The neutron and beta signals from the preamplifiers are amplified, sent through discriminators and multiscaled in separate multichannel analyzers. P_n values and half-lives of the isotopes are determined by analyzing the decay curves obtained by a least squares computer code. The P_n values obtained so far were normalized to an average experimental P_n value of ^{94}Rb compiled from other measurements⁽¹⁾ and are presented in Table 1, together with the measured half-lives.

The absolute efficiency of each counter is a crucial factor in the determination of the P_n values. Hence the counters will be carefully calibrated using calibrated sources prepared by photoneutron reactions.

* Weizmann Institute of Science, Rehovot

** Technion, Israel Institute of Technology, Haifa

TABLE 1
Delayed neutron emission probabilities (P_n) and
half-lives of heavy isotopes of Rb and Cs

Precursor nucleus, Rb	P_n (%)	Half-life (sec)	Precursor nucleus, Cs	P_n (%)	Half-life (sec)
93	1.70 ± 0.20	5.74 ± 0.08	142	0.065 ± 0.009	1.75 ± 0.06
94	9.5 ± 0.99	2.76 ± 0.03	143	1.70 ± 0.020	1.83 ± 0.04
95	5.79 ± 0.65	0.40 ± 0.01	144	-	1.03 ± 0.02
96	9.88 ± 1.20	0.225 ± 0.01			
97	17.80 ± 2.10	0.233 ± 0.019			
98	14.4 ± 1.80	0.105 ± 0.023			

REFERENCE;

1. Asghar, M., Gautheron, J.P., Bailleul, G., Bocquet, J.P., Greif, J., Schrader, H. and Siegert, G., Nucl. Phys. A247, 359 (1975)

EFFECTIVE CROSS SECTION COMPUTATION IN THE UNRESOLVED RESONANCE REGION

Y. Gur and S. Yiftah

The group effective cross section is usually represented, in the resonance region, by two factors⁽¹⁾: (a) the infinitely diluted cross section and (b) the resonance self-shielding factor, which contains the temperature and mixture effects.

In the heavy isotopes data, the resonance region is divided into two subregions (resolved and unresolved resonances), and different treatments are required for cross section computation in each subregion. In the resolved region one can compute the shielding factor with as many interfering resonances as desired while in the unresolved region, where only statistical parameters are given, simplified models are used⁽²⁾. These models usually assume that the total width of the cold resonance is very small compared with its Doppler width. The condition holds for high energy and high temperature, which is the less interesting case where the shielding factor approaches unity, but it certainly does not hold for ^{235}U , ^{239}Pu and ^{241}Pu in the keV region and below. The models also assume no overlapping between resonances of different (ℓ, j) series and overlapping of two resonances of the same (ℓ, j) series. However, overlapping does occur between more than two resonances in the unresolved region. Hence two questions naturally arise: how many overlapping resonances are to be considered for the computation of a reliable shielding factor and how reliable are the results of the simplified computation.

We performed preliminary computations in this connection as follows. The ladder of resolved resonances was continued into the statistical region by sampling virtual parameters⁽³⁾ and energies from the statistical parameters of ^{241}Pu ⁽⁴⁾. Shielding factors were computed with 3, 5, 7, 11, 15, 19 and 25 interfering resonances for 300K and 1500K in the energy regions 80 - 170eV, 1200 - 1270eV and 210 - 2270eV, using the techniques usually used in the resolved resonance region⁽⁵⁾. Computations were made for the complete ladder (s and p-wave resonances) and for a partial ladder (s-wave resonances

only), and remarkable differences were found. For pure ^{241}Pu (i.e. zero background cross section) representation with up to 3% accuracy, more than 15 interfering resonances are needed, while for diluted ^{241}Pu , (i.e. Background cross section = 100) more than 5 interfering resonances are needed. Examination of temperature effects shows that 5 interfering resonances are not enough, and that with a small number of interfering resonances, the computed negative coefficients for the 100eV energy interval tend to increase by up to 10%, predicting too large a contribution of that region to the negative Doppler coefficient.

The same computations will be performed with at least two more ladders of virtual parameters sampled from the same statistical parameters. Then the quality of the simplified model computation⁽²⁾ will be examined by comparing those results with ours. We plan to do similar computations also for ^{235}U and ^{239}Pu .

REFERENCES:

1. Bondarenko, I.L, et al., Group Constants for Nuclear Reactor Calculations, Consultant Bureau, N.Y., 1964.
2. Broeders, I. and Krieg, B., MIGROS-3, KFK 2388, 1977.
3. Gur, Y., NASIF-3, Adaptation of NASIF to statistical ladder sampling, 1978, unpublished.
4. KEDAK-3, Nuclear data tape, Kernforschungszentrum, Karlsruhe.
5. Gur, Y. and Yiftah, S., IA-1292, 1973.

DETERMINATION OF GIANT DIPOLE RESONANCE PARAMETERS OF NUCLEI FROM PHOTON SCATTERING MEASUREMENTS

T. Bar-Noy and R. Moreh

The giant dipole resonance (GDR) of deformed nuclei is usually described by two Lorentzian curves characterized by the peak energies (E_1, E_2), the peak cross sections (σ_1, σ_2) and the widths (Γ_1, Γ_2). In the present work, the GDR parameters for several nuclei were extracted from data on elastic and Raman photon scattering measurements carried out at six discrete energies in the 7.9 - 11.4 MeV range. In doing so, we have assumed the validity of the simple rotator model (SRM) for describing the elastic and Raman scattering cross section in deformed nuclei⁽¹⁾. The values of the GDR parameters extracted in the present work are believed to be more accurate and are essentially free from inaccuracies encountered in direct photonuclear measurements.

TABLE 1

GDR parameters for nuclei in the range $A = 159-238$
as extracted from photon scattering data

Nucleus	E_1 (MeV)	Γ_1 (MeV)	σ_1 (mb)	E_2 (MeV)	Γ_2 (MeV)	σ_2 (mb)	P	β
U	10.87	2.55	322	14.14	4.85	416	2.5	1.3
Th	11.19	3.30	288	14.42	5.31	371	2.1	1.4
Np	10.86	2.91	271	14.26	4.56	426	2.5	1.3
Ta	12.49	2.62	253	15.38	4.29	302	2.0	1.2
Lu	12.09	2.28	240	15.63	4.95	261	2.4	1.1
Ho	12.22	2.66	226	15.65	4.84	247	2.0	1.2
Tb	11.93	3.16	177	15.93	5.44	215	2.1	1.2

This is because in the $A \sim 180$ and $A > 230$ regions, large uncertainties occur in photonuclear cross section. Such deviations are particularly large in the $A > 230$ region due to the effect of photofission and background neutrons.

The accuracy of the present method stems from the fact that the photon scattering cross sections are highly sensitive to small variations of the GDR parameter values. For instance a 10%-15% variation in such parameters causes a factor of $\sqrt{2}$ -3 deviation of the calculated photon scattering cross sections. Table 1 shows the values of the GDR parameters obtained by a minimization procedure on our photon scattering data⁽¹⁻³⁾ for nuclei in the range $A = 159-238$. An interesting result of this procedure is that the present results yield GDR parameters which fall between those obtained by others via (γ, n) measurements. The present parameters reproduce meaningful values of P , the area ratio of the two resonances, and of $\beta = \frac{1}{2}\pi(\sigma_1\Gamma_1 + \sigma_2\Gamma_2)/(0.06 NZ/A)$, the amount by which the integrated cross section exceeds the classical dipole sum-rule.

REFERENCES:

1. Bar-Noy, T. and Moreh, R., Nucl. Phys. A 229 417 (1974)
2. Bar-Noy, T. and Moreh, R., Nucl. Phys. A 275 151 (1977)
3. Bar-Noy, T. and Moreh, R., Nucl. Phys. A 288 192 (1977)

ELASTIC AND RAMAN SCATTERING OF 8.5 - 11.4 MEV PHOTONS FROM ^{175}Lu AND ^{181}Ta (1)

T. Bar-Noy and R. Moreh

Differential cross sections for elastic and inelastic Raman scattering from ^{175}Lu and ^{181}Ta were measured. Five photon energies between 8.5 and 11.4 MeV were used and were obtained from the (n, γ) reaction on Ni and Cr using thermal neutrons. The results were compared with calculations of a modified simple rotator model of the giant dipole resonance (GDR) in which the effect of Delbruck scattering was incorporated. In general, a fair agreement between theory and experiment was obtained. A new set of GDR parameters was extracted, based on photon scattering data, and as expected, yielded better agreement between experimental and predicted cross sections.

REFERENCE:

1. Bar-Noy, T. and Moreh, R., Nucl. Phys. A 288, 192 (1977)

INTERFERENCE BETWEEN NUCLEAR RESONANCE AND NUCLEAR THOMSON SCATTERING OF PHOTONS⁽¹⁾

Z. Berant and R. Moreh

According to theory the real parts of the nuclear resonance (NR) and nuclear Thomson (NT) scattering amplitudes are in antiphase in the energy region below the peak of the giant dipole resonance (GDR). One therefore expects a destructive interference effect between the two scattering processes. Such an effect should reveal itself experimentally as a decrease in the elastic scattering cross section with increasing energy in the range far below the peak of the GDR (Fig. 1). Note that the pure NT scattering contribution is independent of energy and the pure NR scattering contribution increases with energy following a Lorentzian tail.

The observation of this effect is difficult not only because of the smallness of the photon scattering cross sections at the energy region of interest but also because of the ambiguity introduced by Delbruck scattering. Here, we have nearly isolated the coherent contribution of NT and NR scattering by choosing a medium-Z target, ⁵⁵Mn, and by working at $\theta = 140^\circ$ such that the Delbruck contribution was small ($<10\%$) and that of Rayleigh scattering was negligible.

Experimentally, the photon beam was obtained from thermal neutron capture on a set of metallic discs of either vanadium, chromium or nickel. Each set of discs was placed along a separate tangential beam tube of the IRR-2 reactor. This particular choice of the sources was made because the V(n, γ) source yields several well separated strong γ lines between 5.5 - 7.2 MeV, the Cr(n, γ) source has γ lines in the range 7.4 - 9.7 MeV and the Ni(n, γ) source⁽²⁾ has a weak γ line ($\sim 10^5$ photons $\text{cm}^{-2} \text{s}^{-1}$) at $E=11.4$ MeV. In this manner, we covered part of the interesting energy region where a strong interference effect between NR and NT scattering was expected.

The scattered signals from the γ lines having $E = 5.5 - 9.7$ MeV photons were measured with a 40cm^3 Ge(Li) detector while the very weak

signal from the $E = 11.4$ MeV line could be detected only by using a large volume ($12.7 \times 12.7 \text{ cm}^2$) NaI detector. The cross sections are given in Fig. 1. The error includes statistics and that due to geometry.

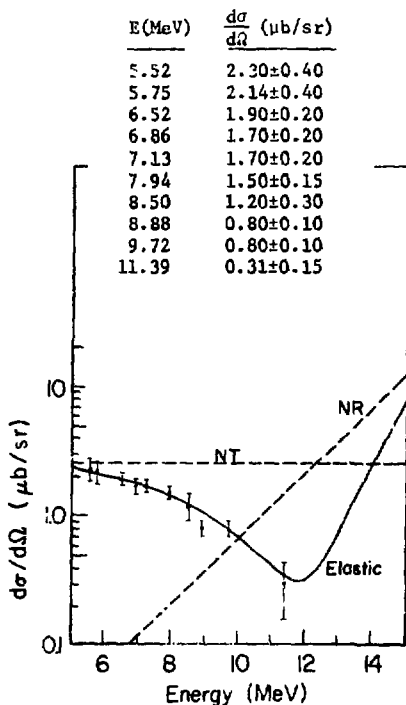


Fig. 1

Differential cross sections ($\mu\text{b}/\text{sr}$) for elastic scattering of photons from ^{55}Mn at $6 = 140^\circ$. The solid curve represents the values obtained by including the incoherent and coherent contributions of NT, NR and D scattering amplitudes. The broken curves represent the pure contributions of nuclear Thomson and nuclear resonance scattering, respectively

The excellent agreement between the theoretical and measured cross sections (Fig. 1) may be viewed as strong experimental evidence for the destructive interference effect. It also shows that the NR amplitudes can well be obtained from an extrapolation of the GDR to the energy region far below the photonuclear emission threshold.

REFERENCES:

1. Berant, Z. and Moreh, R., Phys. Lett. 73B, 142 (1978)
2. Moreh, R. and Bar-Moy, T., Nucl. Instrum. Methods 105, 557 (1972)

STUDIES OF NUCLEAR LEVELS AROUND 7.4 MeV USING A HIGH RESOLUTION γ -MONOCHROMATOR⁽¹⁾

I. Jacob, P. Moreh and A. Wolf

A variable-energy γ source was obtained by nuclear resonance scattering of neutron-capture γ -rays through various scattering angles. An energy resolution of less than 10^{-6} was obtained. Pb and Cd targets were employed to scatter the 7.279 and 7.632 MeV photons, respectively, of the neutron capture γ -rays of Fe. Variation of the angle of the resonantly scattered photons between 60° and 150° permits an energy scan of ~ 370 eV (for Pb) and ~ 760 eV (for Cd) in any absorber. Thus nuclear energy levels in ^{139}La , Ce, Cd and ^{209}Bi absorbers were photoexcited and the corresponding values of $g\Gamma_0$ were extracted from the measured absorption curve.

REFERENCE:

1. Jacob, I., Moreh, R. and Wolf, A., Nucl. Phys., A291 1 (1977)

KINETIC ENERGY OF VIBRATION OF ^{15}N IN BN AND NH_4Cl : THEORETICAL INTERPRETATION

O. Shahaï and R. Moreh

The vibrational kinetic energy of ^{15}N in BN and NH_4Cl as a function of temperature was calculated using the methods of lattice dynamics. In the case of NH_4Cl , the average kinetic energy per degree of freedom of ^{15}N was calculated using the frequency distribution function $g(\nu)$. This function was extracted from the work of Cooley⁽¹⁾ who obtained the dynamic matrix for the case of NH_4Cl after analyzing some experimental data, such as those of inelastic neutron scattering and infrared spectroscopy. It was thus possible to obtain the normal modes of vibration, the normal

frequencies and the fraction of the kinetic energy shared by ^{15}N in NH_4Cl . The situation for BN is slightly different because no neutron scattering data is available (due to the high neutron absorption cross section of ^{10}B). Instead, the function $g(\nu)$ was taken from the data of graphite which has a similar crystallographic structure to BN. A scaling factor, determined empirically, was applied to $g(\nu)$ to account for the different atomic masses in BN and graphite. It was also assumed that the kinetic energy of B and N, in each normal mode, is distributed according to their mass ratio. Using the above procedure, excellent agreement was obtained between the experimental and calculated values of the photon scattering cross section throughout the entire temperature range. The results are illustrated in Fig. 2.

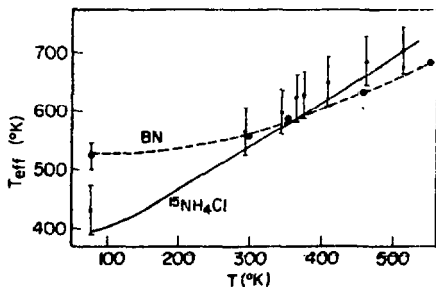


Fig. 2.

The effective temperature, T_{eff} , of ^{15}N as a function of temperature, for both BN and $^{15}\text{NH}_4\text{Cl}$ targets. The curves are the theoretical values obtained as described in the text.

REFERENCE:

1. Cowley, E.R., Phys. Rev. B 3, 2743 (1971)

ZERO-POINT VIBRATIONAL KINETIC ENERGY OF ^{15}N IN BN AND NH_4Cl USING NUCLEAR PHOTON SCATTERING

O. Shahal and R. Moreh

The nuclear resonance scattering cross section of $\sim 6\text{MeV}$ photons generated by neutron capture is dependent on ϵ , the average kinetic energy per degree of freedom of the scattering nucleus (including its zero-point energy) and hence on the Doppler width Δ of the nuclear level. Here, free recoil of ^{15}N occurs and Δ is given by $\Delta = \sqrt{2\epsilon/Mc^2}$ where E is the level energy and M the nuclear mass. It turns out that in strongly bound molecules, the contribution of the zero-point vibration of the atom to its kinetic energy (at 300°K) is usually larger than that of its thermal motion. This fact was nicely illustrated in the results of a study of the temperature variation of the photon scattering cross section from the 6.324 MeV level of ^{15}N using BN and NH_4Cl targets in the range $80^\circ - 600^\circ\text{K}$. The photons were produced by the $\text{Cr}(n,\gamma)$ reactions using thermal neutrons. By knowing the radiative width of the 6.324MeV level in ^{15}N and its energy separation from the incident γ line (1) , it was possible to obtain the values of Δ and hence of ϵ versus the target temperature. The average zero-point kinetic energy per degree of freedom of molecular vibration of ^{15}N was thus deduced by extrapolating the above data to 0°K :

$$\epsilon_0(\text{BN}) = (520 \pm 10)^\circ\text{K}. \quad \epsilon_0(\text{NH}_4\text{Cl}) = (390 \pm 30)^\circ\text{K}.$$

REFERENCE:

1. Moreh, R., Shahal, O. and Volterra, V., Nucl. Phys. A262, 221 (1976)

COULOMB CORRECTION EFFECTS IN DELBRUCK SCATTERING OF 9.0 AND 7.9 MeV PHOTONS ON ^{238}U

S. Kahane and R. Moreh

The elastic differential scattering cross section of 9.0 MeV photons by ^{238}U was measured at $\theta = 1.2^\circ, 1.5^\circ, 25^\circ, 35^\circ, 45^\circ, 60^\circ, 75^\circ, 90^\circ, 120^\circ, 140^\circ$. The results show good agreement with theoretical calculations at

$\theta = 1.2^\circ, 1.5^\circ$ and a large deviation at $\theta \geq 25^\circ$. These results together with data at $E \sim 7.9\text{MeV}$ in U were compared with similar data in ^{181}Ta and strong evidence for the contribution of Coulomb corrections to Delbruck scattering was obtained.

NUCLEAR THOMSON SCATTERING OF 5.5-7.2 MeV PHOTONS⁽¹⁾

Z. Berant, R. Moreh and S. Kahane

Nuclear Thomson (NT) scattering of photons is the analog of the classical Thomson scattering of light by electrons. In the classical picture of this process, the nuclear charge and the center of mass of the whole nucleus oscillate in the same frequency as that of the electric field of the incident radiation. No disruption of the internal coordinates of the nucleons occurs and the differential cross section of NT scattering⁽²⁾ is given by

$$\frac{d\sigma(\theta)}{d\Omega} = \left(\frac{Z^2 e^2}{Mc^2} \right)^2 \left(\frac{1 + \cos^2 \theta}{2} \right) \quad (1)$$

where ze and M are the charge and mass of the nucleus. The experimental test of the above formula in the $\sim 6.5\text{MeV}$ region is difficult not only because $d\sigma/d\Omega$ is small (of the order of $0.7\mu\text{b}/\text{sr}$ for $Z=12$) but also because the photon elastic cross section is a coherent superposition of four scattering processes: NT, nuclear resonance (NR), Raleigh (R), and Delbruck (D) scattering.

Here, we have nearly isolated the NT contribution by choosing low-Z targets (C and Mg) and working at $\theta=140^\circ$ such that the contribution of all other scattering processes is small ($\sim 15\%$) at $E \sim 6.5\text{ MeV}$.

Experimentally, the photon beam was obtained from the $V(n,\gamma)$ reaction on six separated metallic discs (15mm thick by 8.0cm diameter) placed along a tangential beam tube of the IRR-2 reactor.

The theoretical and measured elastic cross sections are compared in Table 1. The effect of including the D contribution is to increase the cross sections by $\sim 4\%$ in both C and Mg. The theoretical values

(Table 2) are lower than the pure NT scattering value because of the destructive interference between NT and NR scattering processes. The magnitude of this effect increases with energy because the contribution of NR becomes larger. The present results are in good agreement with theory as may be seen from Table 2 where the predicted values are well within the error bars of the measured values.

TABLE 2

Differential cross sections ($\mu\text{b}/\text{sr}$) for elastic scattering from C and Mg targets at an angle of 140° . The theoretical values include the combined effect of NT, NR and D scattering; the R contribution was ignored. The values for pure NT scattering are also given

E (keV)	C (Z=6)			Mg (Z=12)		
	Experiment	Theory	Thomson	Experiment	Theory	Thomson
5516	0.17 ± 0.04	0.16	0.17	0.64 ± 0.15	0.61	0.67
5752	0.20 ± 0.06	0.15	0.17	0.66 ± 0.15	0.61	0.67
6465	0.17 ± 0.04	0.15	0.17	0.64 ± 0.15	0.59	0.67
6517	0.16 ± 0.04	0.15	0.17	0.63 ± 0.15	0.59	0.67
6874	0.18 ± 0.04	0.15	0.17	0.59 ± 0.15	0.58	0.67
7163	0.16 ± 0.04	0.14	0.17	0.50 ± 0.15	0.57	0.67

REFERENCES:

- Berant, Z., Moreh and Kahane, S., Phys. Lett. 69B, 281 (1977)
- Alvarez, L.W. Crawford, F.S. and Stevenson M.L., Phys. Rev. 112, 1267 (1958)

MEASUREMENTS OF g-FACTORS OF ISOMERIC STATES IN FISSION FRAGMENTS^(1,2)

A. Wolf and E. Cheifetz*

The inherent alignment of the fragments from spontaneous fission of ^{252}Cf was used to measure the sign and magnitude of g-factors of isomeric states in prompt fission products. The time-differential perturbed angular correlation method was used; the external magnetic field was 7.57 kGauss.

*Weizmann Institute of Science, Rehovot

The advantages of this method are: (a) measurement of g-factors of excited states in neutron-rich nuclei; (b) several g-factors can be measured simultaneously in a multi-parameter experiment. The results are summarized in Table 3.

TABLE 3
g-Factors of isomeric states measured
in this work

Isotope	E_{γ} (keV)	$T_{1/2}$ (nsec) (3)	g
^{107}Mo	65.4	238	-0.92 ± 0.03
^{108}Tc	153.9	108	0.50 ± 0.04
^{109}Ru	96.1	544	-0.22 ± 0.01
^{134}Te	115.3	163	0.846 ± 0.025

The isomeric state in ^{134}Te is known to be a 6^+ state, composed predominantly of two protons in a $(g_{7/2})^2$ configuration coupled to a double magic core. The measured g-factor is significantly above the Schmidt value, and is close to effective g-factors of $g_{7/2}$ protons in nuclei with 82 neutrons. The deviation from the Schmidt value was shown to be due mostly to polarization of the $^{132}\text{Sn}_{82}$ core by $g_{7/2}$ protons.

The experimental value of the g-factor of the 6^+ state in ^{134}Te is somewhat higher than the g-factors of the $(7/2^+)$ ground states of $^{133}\text{Cs}_{82}$ and $^{139}\text{La}_{82}$. This fact indicates the existence of blocking of the core polarization by the presence of additional protons in the $g_{7/2}$ orbit.

REFERENCE:

1. Wolf, A., and Cheifetz, E., Phys. Rev. Lett. 36, 1072 (1976)

2. Cheifetz, E. and Wolf, A., 3rd Int. Conf. on Nuclei Far from Stability, Cargese, 1976, CERN 76-13.
3. Clark, R.G., Glendening, L.E. and Talbert, W.L., in Proc. of the 3rd IAEA Symposium on Physics and Chemistry of Fission, IAEA, Vienna, 1974, vol. II, p. 221.

ANGULAR DISTRIBUTIONS OF SPECIFIC GAMMA RAYS EMITTED IN THE DE-EXCITATION OF PROMPT FISSION PRODUCTS OF ^{252}Cf (1)

A. Wolf and E. Cheifetz*

Angular distributions of specific γ -rays emitted in the de-excitation of prompt fission products of ^{252}Cf were measured with respect to the fission direction. A total of 42 angular distributions were measured, 23 of which were of transitions in even-even fragments. The strong anisotropy ($A_2 = 0.4-0.6$) measured for $2^+ \rightarrow 0^+$, $4^+ \rightarrow 2^+$, and $6^+ \rightarrow 4^+$ transitions in $^{138,140}\text{Xe}$ and $^{142,144}\text{Ba}$ provides direct evidence that the angular momentum of the primary fragments is completely aligned perpendicular to the fission axis. Most of the results are consistent with the results of a statistical calculation. The anisotropies measured for some transitions in even-odd fragments were combined with information of other authors in an attempt to determine spins of low-lying levels in these fragments. Finally, it was shown that about 60% of the anisotropy of the gross unresolved γ -ray spectrum measured extensively by others (2) is due to transitions in the ground state band of even-even fragments.

REFERENCES:

1. Wolf, A. and Cheifetz, E., Phys. Rev. C13, 1952 (1976)
2. Skarsvag, K. and Singstad, I., Nucl. Phys. 62, 103 (1965)

DELAYED NEUTRON EMISSION PROBABILITIES OF Rb, Sr, Cs, AND Ba ISOTOPES

G. Engler, E. Ne'eman*, S. Shalev**, M. Shmid and S. Amiel

Delayed neutron emission probabilities for some isotopes of Rb and Cs were previously reported (1). The work on these isotopes is now

* Weizmann Institute of Science, Rehovot

** Technion, Israel Institute of Technology, Haifa

completed and the studies were extended to isotopes of Sr and Ba. Table 4 presents our latest results, compared with the most recent available information on P_n measurements⁽²⁾. The P_n values for $^{97,98}\text{Sr}$, ^{146}Cs , $^{147,148}\text{Ba}$ and ^{147}La were measured here for the first time.

TABLE 4

Delayed neutron emission probabilities (P_n) of heavy isotopes of Rb, Sr, Cs and Ba

Precursor nucleus	P_n (%)		Precursor nucleus	P_n (%)	
	This work	Others ⁽²⁾		This work	Others ⁽²⁾
^{93}Rb	1.97 \pm 0.22	1.32 \pm 0.03	^{142}Cs	0.082 \pm 0.008	
^{94}Rb	11.1 \pm 0.9	9.7 \pm 0.5	^{143}Cs	1.9 \pm 0.2	1.74 \pm 0.12
^{95}Rb	8.16 \pm 0.84	8.5 \pm 0.5	^{144}Cs	4.07 \pm 0.32	2.95 \pm 0.25
^{96}Rb	14.2 \pm 1.2	12.5 \pm 0.9	^{145}Cs	19.5 \pm 1.5	
^{97}Rb	32.5 \pm 3.5	25.2 \pm 1.8	^{146}Cs	14.1 \pm 1.4	
^{98}Rb	16.7 \pm 1.6	18.4 \pm 2.9	^{147}Ba	5.21 \pm 0.52	
^{97}Sr	0.27 \pm 0.09		^{148}Ba	23.9 \pm 2.1	
^{98}Sr	0.36 \pm 0.11		^{147}La	0.50 \pm 0.17	

REFERENCES:

- Engler, G., Ne'eman, E., Shalev, S., and Shmid, M., in: IA-1338, 1977, p. 100.
- Wünsch, K.D. and Wollnik, H., private communication.

FISSION YIELDS AND HALF-LIFE MEASUREMENTS OF INDIUM ISOTOPES AT THE SOLIS
M. Shmid, G. Engler and S. Amiel

The study of fission yields and half-lives of short-lived mass-separated isotopes with a positive surface ionization integrated target-ion source⁽¹⁾ has been in progress since 1975. After completing the measurements of isotopes of Rb, Sr, Cs and Ba⁽²⁾, an effort was made

to extend the measurements to In isotopes whose fission yields have not been previously measured. The In isotopes are of special interest because they are part of the mass chains which lie between the two peaks of the mass distribution in the thermal fission yield of ^{235}U .

Since the measured isotopes of In have very low fission yields and very short half-lives, it was necessary to use the highest available source temperature, i.e., 2100°C, for the measurements. Figure 3 shows

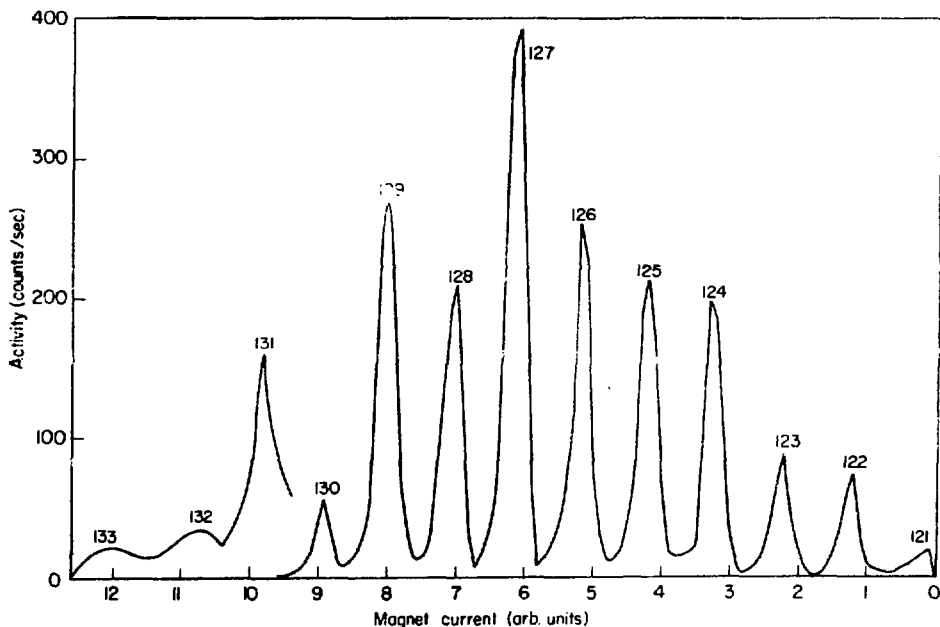


Fig. 3

Beta activity scan over the indium mass range 121-133

a β -activity scan over the mass range 121-133 which was taken with a Si surface barrier detector. Preliminary calculations indicate an enhancement

of the yields of $^{131,132}\text{In}$ in over those predicted by the yield systematics. This may indicate a "wing effect" which was reported for K_B, Sr, Cs and Ba isotopes ⁽²⁾. Half-lives of isotopes of indium were measured. The results are given in Table 5.

TABLE 5
Half-lives of Indium isotopes

Indium Isotope	Half-life (sec)	Indium isotope	Half-life (sec)
123	5.5 \pm 0.5	128	0.84 \pm 0.02
124	3.31 \pm 0.05	129g	0.82 \pm 0.02
125g	2.43 \pm 0.15	130	0.51 \pm 0.02
126	1.48 \pm 0.02	131	0.29 \pm 0.03
127g	0.99 \pm 0.04		

REFERENCES:

1. Shmid, M., Nir-El, Y., Engler, G. and Amiel, S., Nucl. Instrum. Methods 144, 601 (1977)
2. Shmid, M., Nir-El, Y., Engler, G. and Amiel, S., in: IA-1338, 1977 p. 97.

USE OF MAGNETIC FIELDS TO ELIMINATE BETA RAY INTERFERENCE WITH THE MEASUREMENT OF X-RAYS IN NEUTRON ACTIVATED SAMPLES ^{(1)*}

M. Mantel, Z.B. Alfassi and S. Amiel

The study of the possible use of magnetic deflection ⁽²⁾ for the elimination of beta interference in X-rays spectrometry following neutron activation was continued. Theoretical calculations corroborated the experimental results which showed that 3.5-4 kG permanent magnets lowered the background and greatly improved the accuracy of measurements of X-rays

* This work was partially supported by the U.S. - Israel Binational Foundation, Jerusalem

of low and medium Z elements in the presence of strong beta emitters. This effect increases with increasing intensity of the magnetic field. For a 50 μ Ci 32 P source the background is decreased by 99% and 95% for 4.5 and 14keV energies, respectively.

Two practical examples were studied: the determination of copper in hair and of chromium in the presence of phosphates. In both cases the lowered background produced by the magnet makes possible the accurate measurement of the 4.8keV V X-rays and the 7.5keV Ni X-rays obtained from Cr and Cu, respectively, following neutron activation. Without a magnet these low energy X-rays would be completely obscured by the background.

REFERENCES:

1. Mantel, M., Alfassi, Z.B. and Amiel, S. Anal. Chem. 50, 441 (1978)
2. Amiel, S., Mantel, M. and Alfassi, Z.B., J. Radioanal. Chem. 37, 189 (1977)

NONDESTRUCTIVE DETERMINATION OF BROMINE IN BLOOD SERUM BY NEUTRON ACTIVATION AND X-RAY SPECTROMETRY *

M.S. Rapaport, M. Mantel, R. Nothman and S. Amiel

The results obtained by use of magnetic fields to eliminate beta ray interference with the measurement of X-rays emitted from neutron irradiated samples⁽¹⁾ were used for the development of a method for the nondestructive determination of bromine in blood serum.

Beta radiation from the principal components (Na, K, Cl) of blood serum were found to interfere with the nondestructive determination of bromine in this matrix by neutron activation and X-ray spectrometry⁽²⁾.

By applying a magnetic field of 8kG, the background is drastically reduced and the bromine X-rays may be accurately measured. Figure 4 shows the spectra obtained from blood serum samples with and without the application of a magnetic field. From this measurement, a bromine concentration in blood plasma of 12 ± 2 mg/l was found. This amount is in agreement with values mentioned in the literature⁽³⁾.

* This work was partially supported by the U.S. - Israel Binational Foundation, Jerusalem.

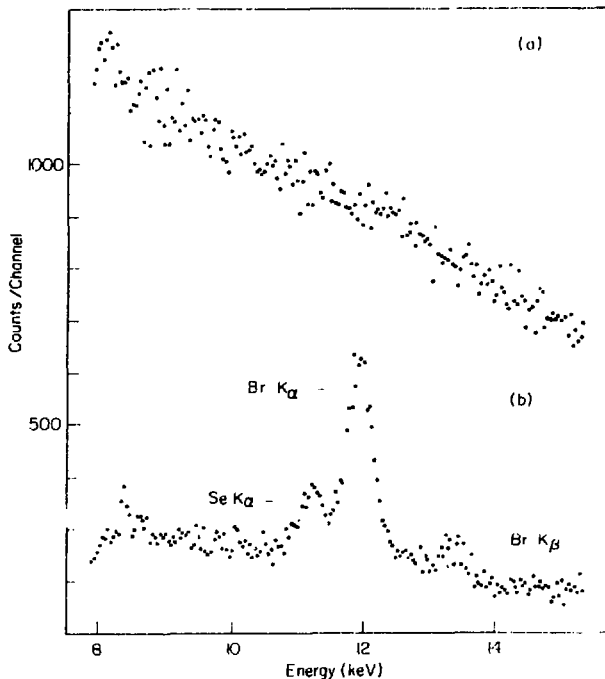


Fig. 4

X-ray spectra of 50λ of blood serum sandwiched between 0.00025 inch thick mylar foils following 20 min irradiation in the rabbit of the IRR-1 reactor. The samples were counted 8 min after the end of irradiation for 1000sec (a) without magnet (b) with an 8kG electromagnet

REFERENCES:

1. Mantel, M., Alfassi, Z.B. and Amiel, S., *Anal. Chem.* 50, 441 (1978)
2. Peisach, M., Maziere, B., Loch, C., Comar, D. and Kellersohn, C., *J. Radioanal. Chem.* 19, 269 (1974)
3. *Biology Data Book*, vol. 3, ed. by P.L. Altman and D.S. Dittmer, Fed. of Amer. Soc. for Expt. Biol., Bethesda, Maryland.

COUPLING CONSTANT SINGULARITIES OF THE NUCLEON-NUCLEON INTERACTION. PART I⁽¹⁾
G. Hazak and A. Gersten*

In a previous paper⁽²⁾ we presented a formalism which permits an exact analysis of the location of coupling constant singular points for approximate Bethe-Salpeter equations with nonlocal pseudopotentials. In the present work the formalism was applied to the interaction of two spin- $\frac{1}{2}$ particles exchanging vector or scalar mesons. (The electromagnetic interaction is a special case.) Analytic expressions for the singular points were obtained. These expressions are independent of the masses and energies of the particles. The physical significance of the singular points was considered.

REFERENCES:

1. Hazak, G. and Gersten, A., Nucl. Phys. A 292, 477 (1977)
2. Gersten, A. and Hazak, G., Nucl. Phys. A 260, 427 (1976)

THERMOLUMINESCENCE IN LiF INDUCED BY MONOENERGETIC, PARALLEL BEAM, 13.8 meV AND 81.0 meV DIFFRACTED NEUTRONS: THE INTRINSIC TL RESPONSE PER ABSORBED NEUTRON^{†(1)}

Y.S. Horowitz*, B. Ben Shahar**+, S. Mordechai*, A. Dubi and H. Pinto

The thermoluminescent response of TLD-600 and TLD-700 to thermal neutrons was measured by exposure to a monoenergetic, parallel beam of 13.8meV and 81.0meV neutrons at the IRR-2 reactor. The measured TLD-600 response for a neutron flux of 10^{10} n/cm² was, after correction for self-shielding, 1470 \pm 90 and 4020 \pm 480 equivalent ⁶⁰Co roentgens at E_n=81.0meV and 13.8meV respectively. These results translate to 2970 \pm 180 and 3350 \pm 400 ⁶⁰Co equivalent roentgens for a maxwellian neutron energy distribution at T=293.6°K. The measured TLD-700 response for a neutron flux

[†]Supported in part by International Atomic Energy Research contract 1614/RB

* Ben Gurion University of the Negev, Beer-Sheva

⁺In partial fulfillment of the requirements for the M.Sc. degree in physics, Ben-Gurion University of the Negev, Beer-Sheva

of 10^{10} n/cm² was 0.12 ± 0.007 ⁶⁰Co equivalent roentgens at $E_n = 81.0$ meV which similarly translated to $0.21_6 \pm 0.012$ equivalent ⁶⁰Co roentgens. These results are accurately corrected for neutron self-shielding and are essentially free of flux depression effects due to neutron backscattering. Monte Carlo calculations were carried out in an attempt to correct previously published results for neutron self-shielding. The neutron induced KERMA is $0.13_5 \pm 0.01$ times as effective as ⁶⁰Co induced KERMA in producing thermoluminescence in TLD-600. This ratio of efficiencies was considered in the framework of the TL-LIF dependence on linear energy transfer.

REFERENCE:

1. Horowitz, Y.S., Ben Shahar, B., Mordechai, S., Dubi, A. and Pinto, H., Radiat. Res., in press.

THERMOLUMINESCENCE IN CaF₂:Dy AND CaF₂:Mn INDUCED BY MONOENERGETIC, PARALLEL BEAM, 81.0 meV DIFFRACTED NEUTRONS⁽¹⁾²

Y.S. Horowitz*, B. Ben Shahar*†, A. Dubi* and H. Pinto

The thermal neutron thermoluminescent response of CaF₂:Dy (TLD-200, 0.35^w/o Dy) and CaF₂:Mn (TLD-400, 2^w/o Mn) was measured by exposure to a monoenergetic, parallel beam of 81.0 meV neutrons at the IRR-2. The TL dosimeters were rectangular, with the following dimensions: 0.165x0.165x0.83 cm. The measured integral TLD-200 response for a neutron fluence of 10^{10} n/cm² was 0.21 ± 0.013 ⁶⁰Co roentgens which translates to 0.33 ± 0.021 ⁶⁰Co roentgens for a maxwellian neutron energy distribution at T=293.6 K. The measured integral TLD-400 response for a neutron fluence of 10^{10} n/cm² was 0.09 ± 0.006 ⁶⁰Co roentgens which similarly translates to 0.14 ± 0.010 ⁶⁰Co roentgens for a maxwellian neutron energy distribution at T=293.6 K. The thermoluminescent response of both materials was theoretically and experimentally shown to be composed of a thermal neutron induced prompt γ component ($\sim 20\%$) and the major component due to the thermal neutron

* Ben Gurion University of the Negev, Beer-Sheva

† This work was performed in partial fulfillment of the requirements for the M.Sc. degree in physics, Ben Gurion University of the Negev, Beer-Sheva

induced beta decay of ^{165}Dy and ^{56}In . It was pointed out that the thermal neutron thermoluminescent response of both materials is size and geometry dependent.

REFERENCE:

1. Horowitz, Y.S., Ben Shazar, B., Dubi, A. and Pinto, H., Phys. Med. Biol., in press.

A STUDY OF HIGH ORDER MODES CONTAMINATION IN 2.43\AA AND 3.83\AA NEUTRON BEAMS USING A PYROLYTIC GRAPHITE FILTER

H. Pinto and H. Shaked

In a previous work⁽¹⁾ the high order modes contamination in a 2.4\AA beam from Al (111) were determined using a 3.18cm pyrolytic graphite (PG) filter. In the present work the high order modes contaminations in 2.43\AA and 3.83\AA beams from a PG (002) monochromator (mosaic spread $3.5\pm 1.5^\circ$) were determined using 5.2cm and 10.4cm PG filters. The results are given in Table 6.

TABLE 6
Composition of the coherently scattered component
in the incident beam (in %)

	2.43\AA		3.83\AA		
	Without filter	5.2cm filter	Without filter	5.2cm filter	10.4cm filter
$\lambda/1$	25.8 ± 0.5	96.0 ± 1.4	5.0 ± 0.8	33.4 ± 2.3	67.1 ± 3.5
$\lambda/2$	56.2 ± 0.9	0.4	34.5 ± 0.4	9.0 ± 2.8	< 1.8
$\lambda/3$	$14.8\pm 1.$	$2.9\pm 2.$	37.1 ± 2.5	18.8 ± 8.2	< 3.1
$\lambda/4$	3.2 ± 1.2	< 0.7	18.8 ± 1.8	33.3 ± 5.6	22.2 ± 15.0
$\lambda/5$	--	--	4.6 ± 1.7	< 5.5	< 5.8

REFERENCE:

1. Pinto, H. and Shaked, H., Nucl. Instrum. Methods 97 71 (1971)

NUCLEAR RESONANCE FLUORESCENCE IN ^{146}Nd AND ^{154}Sm (1)

Z. Berant, J. Tenenbaum and R. Moreh

The γ rays obtained from the $V(n,\gamma)$ reaction using thermal neutrons were employed to photoexcite levels in ^{146}Nd and ^{154}Sm . Angular distribution and polarization measurements were carried out and the following spins and parities were determined: in ^{146}Nd (keV, J^π): 454, 2; 1778, 2; 7163, 1^- and in ^{154}Sm : 82, 2; 921, 1; 1099, 0; 1178, 2; 1202, (0); 6465, 1^- . By combining the data obtained in the present work with those reported in the literature the following spins in ^{154}Sm were assigned: 1440, 2; 1756, 2; 1922, 2; 1986, 2. The M2/E1 mixing ratio for one primary transition in ^{154}Sm was measured. The widths of the resonance levels were determined to be: in ^{146}Nd , Γ (7163 keV) = 125 ± 50 meV and in ^{154}Sm , Γ (6465 keV) = 105 ± 50 meV.

REFERENCE:

1. Berant, Z., Tenenbaum, J. and Moreh, R., Nucl. Phys. A276, 221 (1977)

EFFECT OF MOLECULAR BINDING ON THE RESONANCE SCATTERING OF PHOTONS FROM THE 6.324 MeV LEVEL IN ^{15}N (1)

R. Moreh, O. Shahal and V. Volterra *

The temperature effect of nuclear resonance scattering from the 6.324 MeV level in ^{15}N was studied as a function of temperature using a gaseous $^{15}\text{N}_2$ and a solid $\text{Li}^{15}\text{NO}_3$ target. The γ source was produced by the $\text{Cr}(n,\gamma)$ reaction using thermal neutrons. In order to reproduce the experimental variation of the scattering cross section versus temperature, the Lamb treatment for metallic elements was generalized to the case of diatomic and more complicated molecules. In $^{15}\text{N}_2$ an effective temperature was defined in which the zero-point energy of vibration of the diatomic molecule was included. In LiNO_3 , an effective temperature was also defined by introducing a modified Debye temperature and accounting for the normal modes of vibration of ^{15}N in the $^{15}\text{NO}_3$ molecule. Excellent agreement between measured and calculated values was obtained. In a way, the present measurement may be viewed as detecting the zero-point vibrations in molecules.

REFERENCE:

1. Moreh, R., Shahal, O. and Volterra, V., Nucl. Phys. A262, 221 (1976)

* Ben Gurion University of the Negev, Beer-Sheva

COMPTON SCATTERING CROSS SECTION OF 6.0 - 9.7 MeV PHOTONS BY POLARIZED ELECTRONS⁽¹⁾
R. Moreh, Y. Birenbaum* and O. Shahal

The polarization-sensitive part of the Compton scattering cross section of circularly polarized photons by electrons polarized along the incidence direction of the photons was measured to an accuracy of ~2%. Photons at energies $E_\gamma = 6.0, 7.64, 9.00,$ and 9.72 MeV were obtained from the (n,γ) reaction on Fe, Ni and Cr using thermal neutrons. The polarized electrons were obtained by magnetizing an iron rod near saturation. The measured scattering cross sections were found to be in excellent agreement with theoretical values.

REFERENCE:

1. Moreh, R., Birenbaum, Y. and Shahal, O., Nucl. Phys. A275, 445 (1977)

ELASTIC AND RAMAN SCATTERING OF 8.5-11.4 MeV PHOTONS FROM ^{159}Tb , ^{165}Ho AND ^{237}Np ⁽¹⁾
T. Bar-Noy and R. Moreh

Differential cross sections for elastic and inelastic Raman scattering from the deformed heavy nuclei ^{159}Tb , ^{165}Ho and ^{237}Np were measured at 5 energies between 8.5 and 11.4 MeV. Angular distributions at 4 angles between 90° and 140° for both elastic and inelastic scattering at 9.0 MeV and 11.4 MeV were also measured. The monoenergetic photons were obtained from thermal neutron capture in Ni and Cr. All the angular distributions and the elastic and Raman scattering at the higher energies were in good overall agreement with the results of a modified simple rotator model of the giant dipole resonance in which the effect of Delbruck scattering was included. The data suggest a trend in both the elastic and Raman scattering at lower energies that is stronger than expected. However, the ratio between the Raman and elastic scattering seems to be in good agreement with theory throughout the entire energy range.

REFERENCE:

1. Bar-Noy, T. and Moreh, R., Nucl. Phys. A275, 151 (1977)

NUMERICAL CALCULATIONS OF IMAGINARY DELBRUCK SCATTERING AMPLITUDES

T. Bar-Noy and S. Kahane

The computation of the imaginary Delbruck amplitudes with the formulae of Constantini et al.⁽¹⁾ gave results whose accuracy is greater by a factor of

* Ben-Gurion University of the Negev, Beer-Sheva

10 than that obtained by Ehlotsky and Sheppey⁽²⁾ and Papatzacos and Mork⁽³⁾. This computation was extended to all angular and energetic regions of interest and hence may be very useful in the interpretation of scattering experiments. For completeness, extensive calculations of the real amplitudes (in the Papatzacos and Mork formalism) were also made.

REFERENCES:

1. Constantini, V. et al., Nuovo Cim. 2A, 733 (1971)
2. Ehlotsky, F. and Sheppey, G.C., Nuovo Cim. 33, 1185 (1964)
3. Papatzacos, P. and Mork, K., Phys. Rev. D 12, 713 (1975)

RAYLEIGH AND DELBRUCK SCATTERING OF 6.8-11.4 MeV PHOTONS AT $\theta=1.5^\circ$ ⁽¹⁾

S. Kahane, O. Shahal and R. Moreh

An absolute measurement of the elastic scattering cross section of monoenergetic photons on Pb and U targets in the range 6.8-11.4 MeV at $\theta=1.5^\circ$ was carried out. Strong evidence for the real Delbruck amplitudes and for the Rayleigh scattering contribution from K, L, and higher-shell electrons was obtained for the first time at such energies and scattering angle.

REFERENCE:

1. Kahane, S., Shahal, O. and Moreh, R., Phys. Lett. 66B, 229 (1977)

DELBRUCK SCATTERING OF 9 MeV PHOTONS FROM TANTALUM⁽¹⁾

S. Kahane, T. Bar-Noy and R. Moreh

The differential elastic scattering cross section of 9.0 MeV photons by ¹⁸¹Ta was measured at angles between 25° and 140° and good agreement was obtained between the measured and predicted values between 35° and 90° . In calculating the theoretical cross sections the coherent scattering contributions of nuclear Thomson, nuclear resonance and Delbruck (D) amplitudes were included, while that of Rayleigh scattering was excluded. The D amplitudes were taken from a recent calculation by Papatzacos and Mork⁽²⁾. Evidence for the contribution of the real D amplitude was obtained.

REFERENCE:

1. Kahane, S., Bar-Noy, T. and Moreh, R., Nucl. Phys., in press.
2. Papatzacos, P. and Mork, K., Phys. Rev. D 12, 713 (1975)

DETECTION OF FAST NEUTRON CONTAMINATION IN PHOTON BEAMS⁽¹⁾

Z. Berant, A. Wolf and R. Moreh

A quick method utilizing the ¹⁹F(n, α)¹⁶N reaction was developed for detecting fast neutron contamination in photon beams. A teflon (CF₂)_n target

is used and the 6.131 MeV γ line following the β -decay of ^{16}N is detected using a Ce(Li) detector. The advantages of the present method were considered in comparison with other methods utilizing fast neutron activation, such as $^{27}\text{Al}(n,\alpha)^{24}\text{Na}$ or inelastic neutron scattering e.g. the $^{12}\text{C}(n,n'\gamma)^{12}\text{C}$ reaction.

REFERENCE:

1. Berant, Z., Wolf, A. and Moreh, R., Nucl. Instrum. Methods 140, 109 (1977)

IMPROVEMENT OF THE INTEGRATED TARGET-ION SOURCE OF THE SOLIS

M. Shmid, Y. Nir-El, G. Engler and S. Amiel

The previously reported^(1,2) integrated target-ion source assembly of the SOLIS was further developed for routine operation at temperatures as high as 2100°C. This was achieved by reducing the volume of the tantalum target chamber of the source by about 75%.

It was found that the delay time between production and release of the ionized fission-produced nuclides from the source could be represented by a single time exponent. This was justified theoretically by Rudstam⁽³⁾ in his studies on the mechanisms which govern the release of particles from an ion source assembly.

The most important feature of the present version of the target-ion source is the high efficiency of release of the alkaline earth elements Sr and Ba, which was achieved because of the higher operating temperatures and the use of a Re ionizer. Whereas in the previous version^(1,2) the delay half-time was in the range of 250 sec., it was reduced to about 1 sec with the present source. This drastic reduction in the delay half-time permitted the measurement of isotopes with masses up to 149. The delay half-times of Rb and Cs were also remeasured and determined to be 0.27 sec compared with 0.5 sec previously.

The very short delay half-times facilitated the separation and measurement of short-lived activities of $^{91-98}\text{Rb}$, $^{94-98}\text{Sr}$, $^{96-98}\text{Y}$, $^{140-146}\text{Cs}$, $^{143-149}\text{Ba}$ and $^{144-149}\text{La}$ with half-lives down to 0.1 sec. The preliminary half-lives of ^{149}Ba and its decay products were found to be: 0.2 sec for ^{149}Ba , 1.2 sec for ^{149}La and 4.7 sec for ^{149}Ce . This is the first time that activities of mass 149 are reported.

REFERENCES:

1. Amiel, S., Engler, G., Ne'eman, E., Nir-El, Y. and Shmid, M., in: IA-1321, 1975, p.123.
2. Amiel, S., Engler, G., Nir-El, Y. and Shmid, M., Nucl. Instrum. Methods 139, 305 (1976)
3. Rudstam, G., The Swedish Research Council's Laboratory Report LF-65, 1975.

EVALUATION OF ^{237}Np MICROSCOPIC NEUTRON DATA**

M. Caner[†], S. Wechsler* and S. Yiftah^{†*}

[†]Soreq Nuclear Research Center, Yavne

*Dept. of Nuclear Engineering, Technion, Haifa

ABSTRACT

An evaluation has been done from 10^{-3} eV to 15×10^6 eV of the following ^{237}Np neutron cross sections: total, elastic, radiative capture, fission, total inelastic, partial inelastic, (n,2n), (n,3n) and differential elastic. The number of neutrons per neutron-induced fission and the average elastic scattering cosine in the lab system have been evaluated also.

In the fast neutron energy range, the experimental data are supplemented by optical model and statistical theory calculations.

The recommended data are compared with the ENDF/B-IV file (MAT 1263).

*This research is partly supported by the GfK, Kernforschungszentrum, Karlsruhe.

U N I V E R S I T I E S

GAMMA RAYS DOSIMETRY BY SOLUTIONS OF CHOLESTERIC LIQUID CRYSTALS

ZEEV B. ALFASSI, LIVIU FELDMAN[†] and ABRAHAM P. KUSHELVEISKY

Department of Nuclear Engineering, Ben-Gurion University of Negev, Beersheva, Israel, and

Department of Nuclear Chemistry, Soreq Nuclear Research Center, Yavne, Israel

(Received August 3, 1976; in revised form November 19, 1976)

The γ irradiation of organic solutions of Cholesteric Liquid Crystals (CLC) leads to a decrease in the temperature at which CLC films made from these solutions change colours compared to films prepared from the unirradiated solutions. The decrease in the color transition temperature was found to be proportional to the absorbed dose. The proportionality coefficient can be varied by changing the solvent and the concentration of the solute thus making this system suitable for dosimetry over a large range (tens of Krads to tens of Mrads).

REFERENCES

1. G. H. Brown, *Chemistry* 40, 10 (1967).
2. J. L. Fergason, *Sci. Amer.* 211, 76 (August 1964).
3. J. L. Fergason, *App. Optics* 7, 1729 (1968).
4. J. L. Fergason, *Acoustical Holography* 2, 53 (1970) Plenum Press.
5. J. L. Fergason and G. H. Brown, *J. Am. Oil Chem. Soc.* 45, 120 (1968); J. L. Fergason, N. N. Goldberg and C. H. Jones, Technical Report RADC-TR-64-569, August 1965.
6. J. L. Fergason and N. N. Goldberg, British Patent 1218725 and U.S. Patent 754582, January 1971.
7. A. P. Kushelevski, L. Feldman and Z. B. Alfassi, *Int. J. Appl. Rad. Isot.* in press.
8. T. J. Novak, E. J. Poziomek and R. A. Mackay, *Mol. Crystals and Liq. Crystals* 20, 203 (1973).

NMR STUDY OF THORIUM HYDRIDES ($\text{Th}_4\text{H}_{15}, \text{ThH}_2$) AND DEUTERIDE (Th_4D_{15})

M. Peretz, D. Zamir
Soreq Nuclear Research Centre, Yavne, Israel

and

Z. Hadari
Nuclear Research Centre - Negev, Israel
and Ben Gurion Univ. of the Negev, Beer-Sheva, Israel

ABSTRACT

Thorium hydride was studied using the NMR technique. Relaxation times of protons and deuterons in Th_4H_{15} and Th_4D_{15} were measured over a wide temperature range. Different diffusion processes in different temperature regions were observed. In the range $417 \leq T(^{\circ}\text{K}) \leq 526$ the activation energy for hydrogen (or deuterium) diffusion was calculated to be $E_a = 14.7$ kcal/mole. The preexponential factor τ_0 was calculated to be $\tau_0 \approx 10^{-14}$ sec for hydrogen, and $\tau_0^{\text{D}} = \sqrt{2} \tau_0^{\text{H}}$ for deuterium. The frequency of the quadrupole interaction of the deuterons ν_Q was found to be in the range $37.4 \leq \nu_Q \leq 43.2$ kHz.

The electronic contribution to the relaxation in samples of ThH_2 and Th_4H_{15} was calculated from spin-lattice relaxation time measurements at low temperatures ($78^{\circ}\text{K} \leq T \leq 300^{\circ}\text{K}$). While in ThH_2 this contribution can be given as $(T_1 T)_e = 567 \pm 30$ (sec $^{\circ}\text{K}$) in the above temperature range, that of Th_4H_{15} has been found to be temperature dependent. Analysis of this temperature dependence and that of the Knight shift (measured by Lau et al) permitted an estimation of the hyperfine fields of the s and d electrons at the site of the proton. In view of the NMR results it is suggested that f electrons are not present in a significant amount on the Fermi level.

Mössbauer and magnetization studies of the NpM_2Si_2
($M = Cr, Mn, Fe, Co, Ni, Cu$) systems

J. Gal, M.Kroupp, and Z. Hadari
Nuclear Research Center-Negev Beer-Sheva, P.O.B. 9001

I. Nowik
The Racah Institute of Physics, The Hebrew University

Abstract

Magnetization and ^{237}Np Mössbauer studies of the tetragonal NpM_2Si_2 intermetallic compounds were performed. The compounds exhibit a wide variety of magnetic phenomena. $NpMn_2Si_2$ orders ferromagnetically above 300K, and has a magnetic hyperfine interaction of 1840(50) MHz at 4.2 K. All other compounds order antiferromagnetically. The Neel points and the magnetic hyperfine interaction in saturation of the NpM_2Si_2 compounds are 73(3), 87(3), 42(4), 33(3), 43(3) K and 2800(50), 2300(50), 1730(50), 3430(50) MHz for $M = Cr, Fe, Co, Ni, and Cu$, respectively. In $NpCu_2Si_2$, the magnetic phase transition is of the first order.

References

1. I.Felner, I. Mayer, A.Grill, and M. Schieber, Solid State Commun. 16, 1005 (1975).
2. J.Gal, Z.Hadari, U. Atzmony, E.R.Bauminger, I.Nowik and S.Ofer, Phys.Rev.88, 1901 (1973).
3. P.J. Flanders, Rev.Sci.Instrum. 41, 497 (1970).
4. H. Gabriel, Phys. Status Solidi 23, 195 (1967).
5. A.T. Aldred et al., Phys.Rev 10, 1011-1019 (1974), Phys.Rev.B 11, 530 (1975).
6. B.D. Dunlap and G.M. Kalvius, in *The Actinides: Electronic Structure and Related Properties*, edited by A.J. Freeman and J.B.Darby, Jr. (academic, N.Y., 1974), p. 238.
7. J. Gal, Z. Hadari, E.R. Bauminger, I.Nowik, and S.Ofer, Solid State Commun. 13, 647 (1973).
8. B.D. Dunlap and G.H. Lander, Phys.Rev. Lett. 33, 1046 (1975).

4. Sensitivity of Reactivities to Current Cross-Section Libraries: A Case for Adjustment, U. Salmi, J. J. Wagschal, Atara Ya'ari, Y. Yeivin (Hebrew Univ-Israel)

Evaluated neutron cross-section libraries are being continuously reevaluated, and updated versions of libraries such as ENDF/B, UKNDL, and KEDAK, incorporating the most available information, are periodically released. Such major projects, with all the duplication of the enormous effort involved, are still going on strongly because, quoting a most recent report describing such a reevaluation, "... nuclear data measurements have not yet converged to a unique cross-section basis. Thus the evaluators are required to revise their nuclear data libraries from time to time." Rephrasing this somewhat euphemistic quotation more bluntly, it simply means that current libraries are just inadequate for reliable neutron calculations.

To illustrate this seemingly very strong statement, let us consider the very simple critical assembly Jezebel: a bare homogeneous plutonium-alloy sphere of density 15.61 g cm⁻³ and mass 17.02 kg. The experimental error in the value of this critical mass is $\pm 0.6\%$, corresponding to an "experimental" multiplication factor $k = 1 \pm 0.0017$.

We have calculated this parameter very carefully, starting from a given basic library and generating a set of group constants for an energy-group structure appropriate to the fast-spectrum metallic assemblies. The very high approximations that we used in these calculations were essentially equivalent to 53-group S_p P_n calculations with more than an adequate number of radial divisions. We estimate that our k-calculations are accurate to within at least $k = 0.0005$.

It will be convenient to discuss reactivities, i.e., values of $\rho = 1 - k$, rather than multiplication factors, and express their values in milli-k's, namely, in units of 10^{-3} . Thus, the experimental uncertainty in the reactivity of Jezebel is 1.7 mk, and we expect the precision of our calculations to be about 0.5 mk.

Now, the ENDF B-III (1972) reactivity of Jezebel turns out to be 3.81 mk, by no means a satisfactory value. However, the revised plutonium cross sections of ENDF B-IV (1974) already yield $\rho = -0.26$ mk, well within the experimental error. Although it is tempting to speculate that these revised cross sections might have been "tuned" (meaning that the selection among several experimental data sets was biased by the extent to which certain integral data—obviously including the Jezebel experimental reactivity—were reproduced in calculations based on each of these sets), we shall disregard this possibility.

In any case, using other cross-section libraries, the evaluations of which are based on essentially the same "raw" data used in the ENDF B-IV evaluation, we obtain for the Jezebel ρ values which differ from the ENDF B-IV value by up to over 10 mk.

It should be obvious that this discrepancy is just a reflection of the inherent scatter (or systematic errors) characteristic of the methods and techniques applied in neutron cross-section measurements and evaluation. Let us therefore consider the implication of cross-section uncertainties with respect to calculated reactivities.

To this end, we first of all need to define the sensitivity function of the reactivity with respect to a given cross section. This function, $D(E)$, is defined by the relation

$$\delta\rho = \int D(E) \delta\sigma(E) dE,$$

which relates the change in ρ to the variation of the cross section which induces this change. Let \bar{D} be the average value of $D(E)$ over an energy interval ΔE , and let $\bar{\sigma}$ be the average value of the uncertainty of the cross section under consideration over this energy range. Then, for a rough estimate of the effect on the reactivity ρ over the range ΔE , we have

$$\delta\rho \approx \bar{D}\bar{\sigma}\Delta E.$$

The Jezebel reactivity is most sensitive to the ^{239}Pu fission cross section up to several MeV. For our rough estimate of $\delta\rho$, we consider the range up to 1 MeV. The pertinent average sensitivity over this energy range is $\bar{D} \approx 0.25 \text{ b}^{-1} \text{ MeV}$, $\bar{\sigma} \approx 1.6 \text{ b}$, and the estimated relative uncertainty of σ_f is 10^{-1} (Ref. 2). Thus, just because of the uncertainty in the fission cross section alone (within this limited energy range only), the uncertainty in the calculated reactivity is already

$$\delta\rho \approx 0.25 \cdot 1.6 \cdot 0.1 = 0.04$$

or 40 mk (2), which is 24 times the experimental error of 1.7 mk.

Goel and Weller¹ claim that in KEDAK-3, their latest evaluation, the uncertainty of σ_f of ^{239}Pu above 300 keV is reduced to 6%. Furthermore, Greebler et al.² set an uncertainty of 2% for this cross section as a goal for an adequate library. But even with a 2% uncertainty, we shall still have $\delta\rho_{\text{calc}} \approx 5\delta\rho_{\text{exp}}$. What our rough analysis indicates is that a reduction of this uncertainty to 0.5% or less is needed, at least if one wishes to calculate the reactivities of the metallic clean criticals with any confidence.

This, however, does not seem a realistic goal for the foreseeable future; that is, unless we are ready to incorporate valuable experimental integral data in the evaluation process. In other words, adjustment presently seems the only practical procedure capable of significantly improving the accuracy of cross-section libraries.

1. B. GOEL and F. WELLER, KFK-2386 III, Karlsruhe Nuclear Research Centre (1977).
2. P. GREEBLER, B. A. HUTCHINS, and C. L. COWAN, *Nuclear Data B: Reviews*, Vol. 1, p. 17, IAEA, Vienna, (1976).

AUTHOR INDEX

- Altassi, Z.B. 39, 51
Amiel, S. 19, 36, 37, 39, 40, 48
Bar-Nevo, E. 26, 27, 46, 47
Ben-Shahar, B. 42, 43
Berant, Z. 28, 33, 45, 47
Birenbaum, Y. 46
Ceder, H. 16, 17, 49
Cherik, R. 10, 12, 13
Cneifetz, E. 34, 36
Doh, A. 42, 43
Eisen, Y. 10
Engler, G. 19, 22, 36, 37, 48
Eyal, Y. 10, 12, 13
Farbis, A. 11
Feldman, L. 51
Freundl, Z. 9, 10, 11, 12, 13
Gal, J. 53
Gayer, A. 9
Gershon, A. 42
Goldring, G. 3, 11
Gur, Y. 17, 24
Hadar, Z. 52, 53
Hajak, G. 42
Hilman, M. 10
Horowitz, Y.S. 42, 43
Ilberg, D. 15
Jacob, I. 30
Kahane, S. 32, 33, 46, 47
Kroup, M. 53
Kushlevsky, A. 51
Lavi, N. 71
Lederberger, T. 11
Mantel, M. 39, 40
Mordechai, S. 42
Moreh, R. 26, 27, 28, 30, 32, 33, 45, 46, 47
Ne'eman, E. 22, 36
Nir-El, Y. 19, 21, 22, 48
Notman, R. 40
Nowik, I. 53
Paltiel, Z. 11
Pauli, H.C. 11
Peretz, M. 52
Pinto, H. 42, 43, 44
Rapaport, M.S. 40
Ronen, Y. 18
Salmi, U. 54
Saphier, D. 15
Shaked, H. 44
Shalal, O. 30, 32, 45, 46, 47
Shalev, S. 15, 22, 36
Shmid, M. 19, 22, 36, 37, 48
Shvarts, D. 18
Stocker, H. 12, 13
Tennenbaum, J. 45
Tserruya, I. 10
Vager, Z. 11
Volterra, V. 45
Wagschal, J.J. 18, 54
Wexler, S. 17, 49
Wolf, A. 30, 34, 36, 47
Ya'ari, A. 54

Yevin, Y. 54

Yiftah, S. 15, 16, 17, 24, 49

Zamir, D. 52

